

Review

# Application, Deactivation, and Regeneration of Heterogeneous Catalysts in Bio-Oil Upgrading

Shouyun Cheng, Lin Wei \*, Xianhui Zhao and James Julson

Agricultural & Biosystems Engineering Department, South Dakota State University, 1400 North Campus Drive, Brookings, SD 57007, USA; shouyun.cheng@sdstate.edu (S.C.); xianhui.zhao.china@gmail.com (X.Z.); James.Julson@sdstate.edu (J.J.)

\* Correspondence: lin.wei@sdstate.edu; Tel.: +1-605-688-4179

Academic Editor: Keith Hohn

Received: 31 October 2016; Accepted: 1 December 2016; Published: 7 December 2016

**Abstract:** The massive consumption of fossil fuels and associated environmental issues are leading to an increased interest in alternative resources such as biofuels. The renewable biofuels can be upgraded from bio-oils that are derived from biomass pyrolysis. Catalytic cracking and hydrodeoxygenation (HDO) are two of the most promising bio-oil upgrading processes for biofuel production. Heterogeneous catalysts are essential for upgrading bio-oil into hydrocarbon biofuel. Although advances have been achieved, the deactivation and regeneration of catalysts still remains a challenge. This review focuses on the current progress and challenges of heterogeneous catalyst application, deactivation, and regeneration. The technologies of catalysts deactivation, reduction, and regeneration for improving catalyst activity and stability are discussed. Some suggestions for future research including catalyst mechanism, catalyst development, process integration, and biomass modification for the production of hydrocarbon biofuels are provided.

**Keywords:** biomass; biofuel; pyrolysis; bio-oil; catalyst; catalytic cracking; hydrodeoxygenation; coking; deactivation; regeneration

---

## 1. Introduction

More than 80% of global energy supplies come from fossil fuels including coal, petroleum, and natural gas [1]. However, environmental issues such as global warming and air pollution due to fossil fuel consumption, growing energy demand, and depletion of fossil fuels have stimulated the demand for renewable liquid fuels [2].

Biomass is a promising eco-friendly alternative source of renewable energy in the context of current energy scenarios [3]. Biomass is a form of carbon-neutral energy because the CO<sub>2</sub> released during its utilization is equal to the CO<sub>2</sub> absorbed from the atmosphere during its growth through photosynthesis. It also has lower contents of sulfur, nitrogen, and heavy metals than coal [4]. Therefore, utilization of biomass-derived fuels is crucial to reducing the carbon dioxide emission and air pollution problems caused by fossil fuels. Compared to fossil fuels, the production of biofuels is more environmentally friendly and sustainable since biomass is readily available, annually renewable, and inexpensive. The challenges of fossil fuel depletion, climate change, and other environmental concerns may be addressed if biomass can be efficiently converted into valuable biofuels and chemicals with a low carbon footprint.

Biomass can be converted to liquid biofuels through thermochemical processes. Within the last decades biomass fast pyrolysis has emerged as one of the most promising processes for thermochemical conversion of lignocellulosic biomass to liquid bio-oils. During pyrolysis, biomass is heated up to 400–650 °C in the absence of air and thus broken down into three products: liquid bio-oil and a small amount of solid bio-char and non-condensable gas (also named syngas). Biomass fast pyrolysis

is a simultaneous mix of dehydration, depolymerization, re-polymerization, fragmentation, and rearrangement. These reactions result in a bio-oil liquid that contains over 300 individual compounds including a large variety of oxygenates that cause many of the negative properties of bio-oil, such as low higher heating value (HHV), high corrosiveness, high viscosity, and instability [5]. These properties greatly limit the application of bio-oil, particularly as transportation liquid fuels. Therefore, crude bio-oil has to be upgraded before it can be used as liquid biofuel for fueling engines.

The purpose of bio-oil upgrading is to refine crude bio-oil into hydrocarbons or other intermediates that can be directly dropped into an existing petroleum refinery for production of “green” gasoline, diesel, or other industrial chemicals. This upgrading process is to remove oxygenated compounds from bio-oil via  $H_2O$ ,  $CO$ , and  $CO_2$  formation while at the same time reducing molecular weight and altering chemical structures. Generally bio-oil upgrading may involve a one pot reaction where simultaneous or tandem multiple reactions of catalytic cracking, hydrodeoxygenation, decarbonylation, decarboxylation, hydrocracking, or hydrogenation occur in one reactor. Different catalysts must be used to produce different targeted products. Each of the individual components in bio-oil may play a certain role in bio-oil upgrading one-pot reactions. A series of consecutive and parallel reactions competing against each other between liquid and gaseous products may occur in a one-pot bio-oil upgrading process. There are various intermediates and products generated simultaneously during bio-oil upgrading. Many of them are reactive. The products from one component may react with products from other components while the mineral compounds like alkali and alkaline earth metals that come from biomass can also act as catalysts. This changes product distribution dramatically and can make one-pot reactions more perplexing. Such complex reaction networks make bio-oil upgrading, product separation or purification very difficult. The competitive reactions and impurities in bio-oil also deactivate the catalysts used in the one-pot reactions. This leads to low carbon conversion efficiency and high processing costs. The processing efficiency of bio-oil upgrading relies heavily upon the activity, selectivity, and energy efficiency of the catalysts used. Catalyst deactivation is one of biggest challenges to developing active stable catalysts.

Catalytic cracking and hydrodeoxygenation have proven to be the most promising for upgrade crude bio-oils into liquid hydrocarbon biofuels. These two methods can effectively reduce the contents of oxygenated compounds while producing high yields of hydrocarbons. Heterogeneous catalysts have achieved great success for petroleum refining and are promising for bio-oil upgrading. The objective of this paper is to address recent advances in the use of heterogeneous catalysts for bio-oil upgrading. Specifically, major issues associated with bio-oil upgrading catalysts such as catalysts deactivation caused by coking, methods for reducing catalyst deactivation, and catalysts regeneration techniques will be addressed.

## 2. Bio-Oil Properties and Compositions

Among the different pyrolysis processes used for biomass conversion, slow pyrolysis is currently the most mature and commercially used pyrolysis technology [6,7]. During slow pyrolysis, biomass is heated to around 500 °C at a slow heating rate up to 20 °C/min and a long vapor residence time (5–30 min). This results in a lower yield of liquid bio-oil (around 30 wt%), higher yields of charcoal (around 35 wt%) and gas products (around 35 wt%) [5,8]. Slow pyrolysis has traditionally been used for the production of charcoal rather than bio-oil or gas [9,10]. Fast pyrolysis of biomass is a promising technology for converting biomass to liquid fuels [11]. Fast pyrolysis produces a high yield of liquid bio-oil (50–75 wt%) at moderate temperatures (400–650 °C), atmospheric pressure, high heating rates (>103 °C/s) and short vapor residence time (<2 s) [12,13]. Biomass fast pyrolysis is generally done in fluidized bed, rotating cones, vacuum or ablative pyrolysis reactors [14]. However, the biomass-derived bio-oil is not suitable for direct application as transportation fuels due to the lower heating value (17.4–32.46 MJ/kg) in comparison with heavy fuel oil (44.17 MJ/kg). The comparison of bio-oil and heavy fuel oil properties are listed in Table 1. The low heating value of bio-oil results from its high water content (12–30 wt%) and oxygen content (19.40–50.30 wt%). Also bio-oil has high

viscosity and acidity. Bio-oil is also unstable, and reactions of oxygen-derived compounds during storage, results in reduced bio-oil quality [15].

**Table 1.** Typical properties of bio-oil and heavy fuel oil.

| Physicochemical Properties        | Bio-Oil           | Heavy Fuel Oil |
|-----------------------------------|-------------------|----------------|
| Water content (wt%)               | 12–30             | 0.10           |
| Carbon (wt%)                      | 41.70–69.50       | 85.60–86.68    |
| Hydrogen (wt%)                    | 5.70–9.40         | 10.30–12.04    |
| Oxygen (wt%)                      | 19.40–50.30       | 0.60–0.65      |
| Nitrogen (wt%)                    | 0–9.80            | 0.60           |
| Sulfur (wt%)                      | 0–0.77            | 2.50           |
| Ash (wt%)                         | <0.25             | 0.04           |
| pH                                | 2.26–4.30         | -              |
| Viscosity (Pa·s)                  | 11.10–62.20@25 °C | 0.23@30 °C     |
| Density (g/mL)                    | 0.98–1.19         | 0.94           |
| Higher heating value (HHV, MJ/kg) | 17.40–32.46       | 44.17          |
| Reference                         | [12,16–24]        | [12,16–24]     |

Pyrolysis bio-oils are complex mixtures containing more than 300 components derived from the depolymerization and fragmentation reactions of cellulose, hemicellulose, and lignin present in biomass [5]. Depending on production conditions, and biomass feedstock type and quality, fast pyrolysis bio-oil composition can vary drastically [25]. The chemical compositions of bio-oils produced from several biomass feedstocks are listed in Table 2. There are many categories of oxygenated compounds present in bio-oil, which include phenols, ketones, aldehydes, acids, esters, furans, ethers, and alcohols. These oxygenated compounds lead to the detrimental properties of bio-oil including high viscosity, corrosiveness, instability, and low heating values [14]. Acids contribute to the corrosiveness of bio-oil, and the presence of aldehydes and phenols results in storage instability [26]. Raw bio-oil requires considerable upgrading to be usable. Two widely investigated methods for upgrading bio-oil into hydrocarbon biofuels are: catalytic cracking and hydrodeoxygenation.

### 3. Catalytic Cracking

Catalytic cracking is an effective bio-oil upgrading method, and it is generally done in the presence of heterogeneous catalysts at atmospheric pressure and at temperatures ranging from 350 °C to 650 °C. Catalytic cracking removes oxygen in the form of CO, CO<sub>2</sub>, and/or H<sub>2</sub>O [27]. The oxygenated compounds in raw bio-oil can be transformed into light hydrocarbon biofuel containing high contents of aromatic hydrocarbons by catalytic cracking. Catalytic cracking can be classified into in-situ and ex-situ processes. In the in-situ process, the biomass and catalysts were mixed together in a single reactor, and this method reduces the capital and operating costs [28]. In the ex-situ process, bio-oil catalytic upgrading is completed in a secondary reactor separate from the biomass pyrolysis reactor. This process enables easier catalyst performance optimization and reduces catalyst to biomass ratio [29,30]. Catalysts include zeolite and oxides. The most recent catalysts used for catalytic cracking are listed in Table 3.

**Table 2.** Typical chemical compositions of bio-oils produced from different feedstocks.

| Feedstock        | Switchgrass<br>(% <sup>1</sup> ) | Rice Husk<br>(%) | Palm Shells<br>(%) | Pine Sawdust<br>(%) | Algae<br>(%) | Corn Stover<br>(wt% <sup>2</sup> ) | Switchgrass<br>(wt%) | Algae<br>(wt%) | Pine<br>(wt%) | Hardwood<br>(wt%) | Softwood<br>(wt%) |
|------------------|----------------------------------|------------------|--------------------|---------------------|--------------|------------------------------------|----------------------|----------------|---------------|-------------------|-------------------|
| Temperature (°C) | 510                              | 450              | 490                | 500                 | 500          | 500                                | 500                  | 360            | 520           | 460               | 510               |
| Phenols          | 18.95                            | 29.20            | 50.44              | 16.98               | 27.93        | 2.39                               | 0.97                 | 1.70           | -             | 1.40–3.90         | 1.40–3.90         |
| Ketones          | 9.86                             | 2.80             | -                  | -                   | 3.16         | 0.20                               | 1.39                 | 1.50           | 5.36          | 0.08–0.96         | 0.02–0.73         |
| Aldehydes        | 10.26                            | 0.00             | 3.42               | -                   | -            | 4.00                               | -                    | -              | 9.73          | 1.03–14.36        | 0.52–0.70         |
| Acids            | 3.25                             | 5.10             | 6.87               | 4.64                | 10.42        | 6.26                               | 10.03                | 0.50           | 5.60          | 3.30–21.50        | 2.20–19.00        |
| Esters           | 4.23                             | - <sup>3</sup>   | -                  | -                   | -            | -                                  | -                    | -              | -             | -                 | -                 |
| Furans           | 7.81                             | 2.30             | -                  | -                   | 6.41         | 0.71                               | 3.38                 | -              | 4.47          | 0.20–1.93         | 0.39–1.83         |
| Ethers           | 9.22                             | -                | 4.51               | -                   | -            | -                                  | -                    | -              | -             | -                 | -                 |
| Alcohols         | 5.66                             | 9.40             | 1.01               | -                   | 0.36         | 7.12                               | 0.64                 | -              | 2.9           | 6.41–7.82         | 1.78–3.17         |
| Others           | 30.76                            | 51.20            | 33.75              | 78.38               | 51.72        | 79.32                              | 83.59                | 96.30          | 71.94         | 49.53–87.58       | 70.67–94.21       |
| Reference        | [19]                             | [31]             | [16]               | [18]                | [21]         | [32]                               | [33]                 | [34]           | [15,35]       | [36]              | [36]              |

<sup>1</sup> peak area; <sup>2</sup> mass percentage; <sup>3</sup> not available.

**Table 3.** Recent advances in heterogeneous catalysts for catalytic cracking of bio-oil and model compounds.

| Catalysts   | Feedstocks   | Temperature<br>(°C) | Reactor Type           | Main Products | Product Yield<br>(wt%)        | Product Compositions<br>(Peak Area %) | Coke Yield<br>(wt%) | Findings  | References    |
|---|--|---------------------|------------------------|---------------|-------------------------------|---------------------------------------|---------------------|---|---------------|
| <b>Zeolite catalysts</b>  |  |                     |                        |               |                               |                                       |                     |   |               |
| HZSM-5, ZnO/HZSM-5, Ga <sub>2</sub> O <sub>3</sub> /HZSM-5, CuO/HZSM-5, Mo/HZSM-5, Cu/HZSM-5, Mo-Cu/HZSM-5, β-zeolite, Co/HZSM-5, Co-Mo/HZSM-5  | Rape straw bio-oil, hydroxypropanone, cyclopentanone, acetic acid, phenol, guaiacol, pine sawdust bio-oil, jatropha bio-oil, prairie cordgrass bio-oil             | 400–600             | Fixed-bed, quartz tube | Hydrocarbons  | 4.58–34.06 (OP <sup>1</sup> ) | 25.71–96.9                            | 0.33–25.07          | HZSM-5 with Si/Al ratio of 50 obtained high oil phase yield.  | [27,30,37–39] |
| Ni/HZSM-5, P/HZSM-5, Zn/HZSM-5, Ti/HZSM-5, Mg/ZSM-5, Ni/ZSM-5, Cu/ZSM-5, Ga/ZSM-5, Sn/ZSM-5, Ultrastable-Y, ZSM-5, Beta-zeolite, Zn/ZSM-5, Zn/Na-ZSM-5, ZSM-5 + SiAl, NiMo/SiAl, Zn/ZSM-5 | Prairie cordgrass bio-oil, rape straw bio-oil, pine wood bio-oil, fallopia japonica bio-oil, camelina oil, carinata oil, jatropha oil, douglas fir sawdust bio-oil | 268.9–600           | Fixed-bed              | Hydrocarbons  | 15.02–82.88 (W <sup>2</sup> ) | 16–93.69                              | 1.1–2.5             | 12% Ni/HZSM-5 yielded the highest amount of gasoline hydrocarbons. Higher reaction temperature is required to maintain zeolite recycle. | [40–48]       |

Table 3. Cont.

| Catalysts  | Feedstocks   | Temperature (°C) | Reactor Type                               | Main Products                               | Product Yield (wt%) | Product Compositions (Peak Area %) | Coke Yield (wt%) | Findings  | References |
|--|--|------------------|--|---|---------------------|------------------------------------|------------------|---|------------|
| H-Mordenite, H-ZSM-5, H-Y, H-Beta, H-Ferrierite, Cu/ $\beta$ -zeolite, Co/ZSM-5, Fe/ZSM-5, Ni/ZSM-5, Ce/ZSM-5, Ga/ZSM-5, Cu/ZSM-5, Na/ZSM-5, CaO/HZSM-5,   | Oak, corn cob, corn stover, switchgrass bio-oil, Japanese knotweed bio-oil, aspen wood bio-oil, cellulose bio-oil, straw lignin bio-oil, corn stover bio-oil | 400–600          | Micro pyrolyzer, fixed-bed, tubular quartz | Hydrocarbons                                | 1–93.30             | - <sup>3</sup>                     | 0.71–31.2        | H-ZSM-5 was most effective for producing aromatic hydrocarbons. Cu doping decreased coke deposit on spent catalyst.                                   | [49–52]    |
| Ga/Meso-MFI, HZSM-5, Meso-MFI, HY, waste FCC   | Radiata pine sawdust bio-oil, wild reed bio-oil  | 500              | Fixed-bed, U-tube quartz                   | Aromatic hydrocarbons, furans, phenolics    | 11.7–15.4 (OP)      | 2–42.7 (wt% <sup>4</sup> )         | 17.3–21.3        | Ga/Meso-MFI increased organic fraction of bio-oil and catalyst resistance to coke deposition.   | [53,54]    |
| <b>Oxides catalysts</b>  |  |                  |  |   |                     |                                    |                  |   |            |
| CaO, MCM-41, MgO, NiO, Al <sub>2</sub> O <sub>3</sub> , FCC, ZSM-5, ZrO <sub>2</sub> /TiO <sub>2</sub> , Silica alumina, MgO, B <sub>2</sub> O <sub>3</sub> , Na <sub>2</sub> CO <sub>3</sub> / $\gamma$ -Al <sub>2</sub> O <sub>3</sub>             | Corn cob bio-oil, beech wood bio-oil, empty palm oil fruit bunch bio-oil, oil palm fronds bio-oil, woody fiber bio-oil                                       | 400–1000         | Thermogravimetric analyzer, fixed-bed      | Aromatic hydrocarbons, phenolics,           | 5.46–37.1 (OP)      | 0–49.8                             | -                | ZrO <sub>2</sub> /TiO <sub>2</sub> and ZSM-5 effectively reduced bio-oil oxygen content. B <sub>2</sub> O <sub>3</sub> promoted cleavage of C–O bond. | [55–59]    |
| Nano MgO, CaO, TiO <sub>2</sub> , Fe <sub>2</sub> O <sub>3</sub> , NiO, ZnO, Zn/Al <sub>2</sub> O <sub>3</sub> , Ce/Al <sub>2</sub> O <sub>3</sub> , Ni/Al <sub>2</sub> O <sub>3</sub> , Mo <sub>2</sub> N/ $\gamma$ -Al <sub>2</sub> O <sub>3</sub> | Poplar wood bio-oil, sunflower stalk bio-oil, lignin bio-oil   | 500–850          | Fixed-bed, pyroprobe pyrolyzer             | Hydrocarbons                                | 6.7–17.5            | -                                  | 5.37–8.59        | CaO greatly reduced acids in bio-oil.   | [60–62]    |
| ZnO, sepiolite, bentonite, attapulgite, red mud, Ce/Al <sub>2</sub> O <sub>3</sub> , Ce/ZrO <sub>2</sub> , Ni–Ce/Al <sub>2</sub> O <sub>3</sub> , Ni–Ce/ZrO <sub>2</sub> , Mg–Ce/Al <sub>2</sub> O <sub>3</sub> , Mg–Ce/ZrO <sub>2</sub>             | Rice husk bio-oil, pine woodchips bio-oil, algae bio-oil   | 400–600          | Auger, fixed-bed                           | Hydrocarbons, phenols                       | 16.77–49.91 (W)     | 6.99–67.98                         | -                | NiCe/Al <sub>2</sub> O <sub>3</sub> produced highest bio-oil yield with the lowest oxygen.  | [63–65]    |
| <b>Other catalysts</b>   |  |                  |  |   |                     |                                    |                  |   |            |
| FCC  | Pine woodchip bio-oil, gas oil   | 540–560          | Fluidized bed                              | Gasoline, light cycle oil                   | -                   | -                                  | -                | Similar product yields were obtained from FCC feed when 10% bio-oil was added.  | [66]       |
| Fe/AC, K <sub>3</sub> PO <sub>4</sub> /Fe <sub>3</sub> O <sub>4</sub>  | Douglas fir pellet bio-oil, poplar wood bio-oil  | 309–591          | Microwave, quartz tube                     | Furans, phenols, guaiacols, ketones, ethers | 23.30–45.20 (W)     | 48.6–87                            | -                | Acid-catalyzed ring opening of furans forms aldehydes.  | [67,68]    |

<sup>1</sup> is oil phase yield; <sup>2</sup> is total bio-oil yield; <sup>3</sup> not available; <sup>4</sup> mass percentage.

### 3.1. Catalysts in Catalytic Cracking

#### 3.1.1. Zeolite Catalysts

Zeolite catalysts have been shown to be effective in the deoxygenation of bio-oil, resulting in the formation of aromatics and effectively increasing the C/O ratio in upgraded bio-oil. Zeolite catalysts such as HZSM-5,  $\beta$ -zeolite, Y-type zeolite, ferrierite zeolite, mordenite zeolite, MCM-41, and SBA-15 have documented use for bio-oil catalytic cracking [37,38,49,55,69,70]. Among these catalysts, HZSM-5 is most effective due to its high activity, strong acidity, and shape selectivity [49,56,71]. HZSM-5 zeolite bio-oil upgrading has effectively transformed bio-oil to liquid biofuel, abundant in aromatic hydrocarbons through deoxygenation, dehydration, decarboxylation, decarbonylation, cracking, oligomerization, alkylation, isomerization, cyclisation and aromatization reactions [72,73]. However, HZSM-5 is easily deactivated by coking, resulting in low yields and short life cycle times.

#### 3.1.2. Oxides Catalysts

Inexpensive oxide catalysts have been widely used as mild catalysts to reduce the oxygen content in bio-oil. Alumina, nickel monoxide, zirconia/titania, tetragonal zirconia, titania, and silica alumina were investigated for use with catalytic pyrolysis of beech wood in a fixed bed reactor at 500 °C [56]. The results indicated that alumina showed the highest selectivity towards hydrocarbons and yielded low organic liquid products. In comparison, zirconia/titania exhibited good selectivity towards hydrocarbons and yielded higher organic liquid product than alumina. Natural derived basic magnesium oxide (MgO) catalyst effectively reduced the oxygen content of the produced bio-oil and exhibited similar or even better catalytic performance in bio-oil upgrading compared to that of an industrial ZSM-5 catalyst, although the coke yield of MgO catalyst was a bit higher than that of ZSM-5 [57]. The reduction of acids and deoxygenation of bio-oils via ketonization and aldol condensation reactions occurred in the basic sites of MgO catalysts, and the preferred pathway for removing oxygen was mainly via CO<sub>2</sub> formation instead of CO and/or water. Zinc oxide (ZnO) catalyst was used for catalytic pyrolysis of rice husks to produce bio-oil in a fixed-bed reactor. ZnO catalyst decreased the amount of undesired oxygenated compounds in bio-oils [63]. Boric oxide (B<sub>2</sub>O<sub>3</sub>) selectively eliminated 50%–80% of the hydroxyl and methoxy groups in the bio-oil produced from empty palm oil fruit bunch and oil palm fronds in a fixed-bed reactor at 400 °C [58]. Boric oxide enhanced the cleavage of C–O bonds in the biomass polymers. This was due to the change of the boric oxide structure from a planar triangular BO<sub>3</sub> to a tetrahedral BO<sub>4</sub> using the oxygen generated from the oxygenated groups in the bio-oil. Nano metal oxides also exhibited good catalytic activity in bio-oil upgrading. For instance, nano MgO, CaO, TiO<sub>2</sub>, Fe<sub>2</sub>O<sub>3</sub>, NiO, and ZnO were used in catalytic cracking of poplar wood pyrolysis vapors in a pyrolysis tube [61]. The results indicated that CaO was the most effective catalyst in increasing the formation of hydrocarbons, reducing the production of anhydrosugars and phenols, and eliminating acids.

### 3.2. Catalyst Deactivation in Catalytic Cracking

Coking is the main reason for catalyst deactivation in catalytic cracking. The results are reduced hydrocarbon yield, catalysts activity, selectivity, and life cycle time by covering active sites on the catalysts and blocking catalysts pores [60]. Coke is a kind of large molecule aromatic compound. Coking increases with increased temperature, especially above 400 °C [74]. Catalyst coke is formed from lignin derivatives and the transformation of bio-oil oxygenates by cyclization, aromatization, and condensation reactions into the olefinic and aromatic heavy components [75]. Lignin derived phenolic, guaiacol compounds, acetic acid, and acetaldehyde are important precursors of coke formation on zeolite catalysts. The acidity (acid strength and number of acid sites) of zeolite catalysts is essential for catalytic deoxygenation, and also plays an important role in catalyst coke formation. Zeolite catalysts with higher acidity were more effective in promoting bio-oil catalytic cracking reactions, but they also

resulted in higher tendencies for coke formation. Therefore, the acidity of zeolites catalysts should be optimized to achieve higher catalyst activity and lower coke formation.

Catalysts coke formation mechanisms have been investigated by many researchers [75–78]. The mechanisms for coke formation during catalytic cracking of methanol and pine sawdust bio-oil over Ni/HZSM-5 catalysts at 450 °C in a fluidized bed reactor was proposed by Valle et al. [76].

Figure 1 is a proposed scheme of chemical reactions for the conversion of a bio-oil/methanol mixture into hydrocarbons and coke using a Ni/HZSM-5 catalyst. All chemical reaction steps shown in the figure occur in a fluidized bed reactor at a temperature of 450 °C and pressure of 0.1 MPa. Apart from the main products (hydrocarbons, C<sub>2–4</sub> olefins, C<sub>5+</sub> aliphatics, C<sub>5+</sub> aromatics, thermal coke and catalytic coke) shown in the figure, some side products including CH<sub>4</sub>, CO, CO<sub>2</sub> and C<sub>2–4</sub> paraffins were also detected.

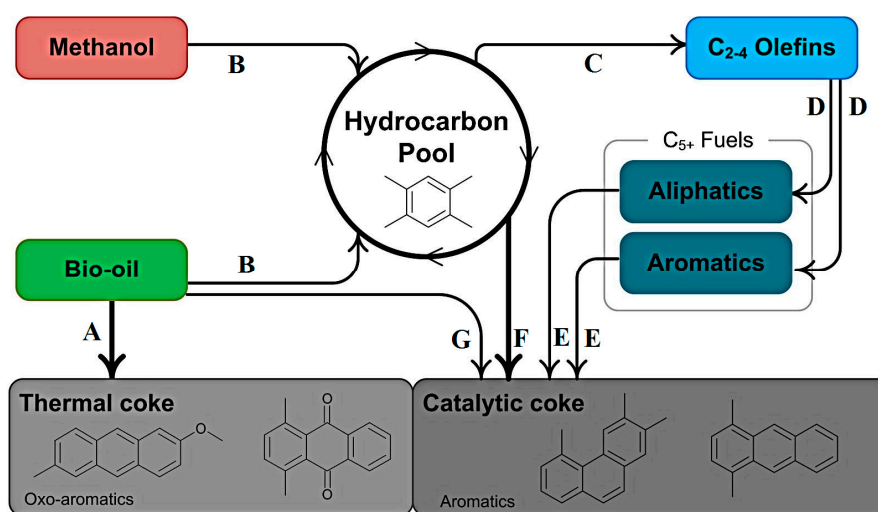


**Figure 1.** The scheme of chemical reactions for the conversion of a bio-oil/methanol mixture into hydrocarbons and coke using a Ni/HZSM-5 catalyst [76]. Copyright 2012, Elsevier.

The coke deposited on Ni/HZSM-5 catalysts consists of thermal coke (mainly located outside of the microporous structure of zeolite) and catalytic coke (mostly located inside HZSM-5 zeolite channels) on Ni/HZSM-5 catalysts. Thermal coke was formed by condensation–degradation and polymerization reactions of bio-oil oxygenated compounds derived from lignin pyrolysis in step A [76]. The methanol and bio-oil mixture was transformed into aromatic hydrocarbons present in the hydrocarbon pool via direct deoxygenation, dehydration, decarboxylation, decarbonylation, and cracking reactions using a Ni/HZSM-5 catalyst in step B [79]. Some hydrocarbons contained in the hydrocarbon pool were transformed to C<sub>2–4</sub> olefins through oligomerization–cracking reactions in step C [80]. C<sub>2–4</sub> olefins were then transformed to C<sub>5+</sub> aliphatics and C<sub>5+</sub> aromatics through alkylation, oligomerization and hydrogen transfer reactions in step D [81]. The C<sub>5+</sub> aliphatics and C<sub>5+</sub> aromatics then undergo rearrangement and condensation reactions to form alkylaromatics and polyaromatics that comprise the catalytic coke in step E [77,79]. Some hydrocarbons present in the hydrocarbon pool were directly converted to catalytic coke through oligomerization, cyclization, aromatization, and condensation reactions that were catalyzed by acid sites of Ni/HZSM-5 catalyst in step F [76]. The condensation and polymerization reactions of the oxygenated compounds in bio-oil also contributed to the formation of catalytic coke in step G [76].

### 3.3. Reducing Catalyst Deactivation in Catalytic Cracking

In order to reduce catalyst deactivation over zeolite catalysts, metal incorporation with zeolites was evaluated during bio-oil catalytic cracking studies. The loading of metal on zeolites improved catalyst selectivity toward aromatic hydrocarbons and reduced coke formation over catalysts. This was

due to the bifunctional activity of the metal modified zeolite catalyst including deoxygenation of zeolite and dehydrogenating of metal species [39,42]. Low concentration Cu-modified  $\beta$ -zeolite (0.5 wt%) increased selectivity to hydrocarbons during catalytic upgrading of Japanese knotweed pyrolysis bio-oil at 600 °C when compared to  $\beta$ -zeolite alone. It also decreased the coke deposition on Cu/ $\beta$ -zeolite catalyst [50]. Nickel substituted HZSM-5 catalyst improved hydrocarbon yield (around 16 wt%) and reduced coke yield during catalytic upgrading of aspen wood pyrolysis bio-oil vapor at 600 °C when compared to HZSM-5 alone [51]. The incorporation of gallium with mesoporous MFI zeolite increased both the organic fraction of the bio-oil and catalyst resistance to coke deposition during catalytic upgrading of pyrolytic bio-oil vapors derived from pine sawdust at 500 °C [53]. The loading of Co and/or Mo with HZSM-5 was found to reduce coke formation and improve hydrocarbon formation when converting prairie cordgrass to hydrocarbon biofuel in a two-stage reactor system [39]. The anti-coking and aromatization performance of zinc and titanium modified HZSM-5 were improved in catalytic transformation of rape straw pyrolysis bio-oil vapor to refined bio-oil [42]. The coke formation over Zn/HZSM-5 during pine sawdust bio-oil upgrading was reduced when compared to pure HZSM-5. This was due to the inhibited coke formation caused by the reduction of the strong acidic sites due to zinc incorporation [48]. In addition, Mg, Ni, Cu, Ga, and Sn-loaded (1 wt%) ZSM-5 zeolites were evaluated during catalytic upgrading of the organic phase of biomass pyrolysis bio-oil at 450 °C [43]. Due to the higher hydrocarbon yield and lower coke yield compared to parent HZSM-5, Ni/ZSM-5 and Sn/ZSM-5 are potential candidates in the catalytic upgrading of pyrolysis bio-oil.

The co-feeding of hydrogen-rich feedstocks is another effective method for reducing coke formation over zeolite catalysts. Co-cracking reactants with high H/C ratios including alcohols, FCC gas oil, low-density polyethylene (LDPE) plastic, H<sub>2</sub>, and steam are effective at suppressing coke formation during bio-oil catalytic cracking [27,82]. The co-cracking of bio-oil with methanol significantly reduced coke deposition on Ni/HZSM-5 catalyst during pine sawdust bio-oil upgrading [76]. This was due to the increased H/C ratio in the feed in the catalytic cracking. Co-processing of bio-oils with vacuum gasoil lowered coke formation over HZSM-5 catalyst during the Fluid Catalytic Cracking (FCC) process [83]. This was due to the restricted access of the oxygenated molecules into the zeolite pores, and coke formation on the outside surface led to pore blocking. Catalytic fast pyrolysis of pine wood and LDPE using ZSM-5 catalyst was investigated at 550 °C [84]. Significant petrochemical production enhancement and coke reduction was observed using a ZSM-5 catalyst. The decreased coke formation was mainly due to hydrogen-transfer reactions between LDPE-derived hydrocarbons and pine wood-derived oxygenates. Co-feeding H<sub>2</sub> into the reactor showed great potential to minimize HZSM-5 catalytic coking [85]. The possible reason was that H<sub>2</sub> played a role in keeping the catalyst surface cleaner and had a moderate effect in hydrogen transfer reactions. This led to the better catalyst stability. Co-processing steam with the bio-oil also reduced the rate of HZSM-5 catalyst deactivation and decreased the total yield of coke and char in bio-oil catalytic upgrading at 340–370 °C [86].

The integration of multiple step bio-oil upgrading processes is beneficial in decreasing the coke formation and improves yields of aromatic hydrocarbons. A two-step catalytic conversion of wood pyrolysis bio-oil to hydrocarbon fuels over HZSM-5 in a dual reactor (low temperature (340–400 °C) and high temperature (350–450 °C)) system was reported by Sharma et al. [87]. The results indicated that the yields of aromatic hydrocarbons produced in the dual reactor system were nearly two-fold compared to those from a single reactor system, and the coke and char yields were much lower (10 wt%) than from those from the single reactor system (29 wt%) at 340 °C. Gayubo et al. also reported a two-step (thermal and catalytic) in-line process for the upgrading of crude bio-oil over HZSM-5 catalyst [88]. The first thermal step separated pyrolytic lignin presented in bio-oil at 400 °C. This produced treated bio-oil that resulted in lower coke deposition over HZSM-5 in catalytic cracking in the second fluidized catalytic reactor. This two-step bio-oil upgrading process reduced catalyst deactivation and avoided blockage of the catalytic bed. A two-stage continuous hydrogenation-cracking reaction process using

Pd/nano-SiO<sub>2</sub> and HZSM-5 catalysts was used to convert model bio-oil compound mixture and ethanol into aromatic hydrocarbons [71]. The results showed that the application of mild hydrogenation before bio-oil cracking significantly reduced the unstable components in bio-oil and thus suppressed coke deposition on HZSM-5.

### 3.4. Catalyst Regeneration and Recycling in Catalytic Cracking

In order to improve catalyst lifetime and reduce operation cost of bio-oil catalytic cracking, repeated catalyst regeneration or recycling becomes an economic necessity. Oxidation regeneration by burning coke at high temperature in air was attempted to recover zeolite catalyst activity [60,73,89]. In order to avoid the irreversible loss of acidity, the catalysts' regeneration temperature should not exceed the catalyst calcination temperature. Repeated fixed bed reactor upgrading–regenerating of HZSM-5 zeolite during upgrading of wood derived pyrolysis oil to aromatic hydrocarbons was reported [73]. The removal of the coke deposited over HZSM-5 was accomplished by burning coke in air at 500 °C for 12 h. However, the recovered HZSM-5 catalyst performance was reduced during five upgrading–regenerating cycles. The loss of catalyst activity was mainly due to the reduced number of Brønsted acid sites responsible for bio-oil upgrading. The loss of acid sites was due to localized temperatures higher than 500 °C. Therefore, in order to avoid hot spots or high temperatures during hot catalyst air regeneration, the coke combustion process might be controlled by initially feeding low concentrations of air using diluents such as nitrogen and steam and then gradually increasing oxygen concentration to complete the coke conversion [90].

In order to improve hydrothermal stability of the HZSM-5 catalyst, a high SiO<sub>2</sub>/Al<sub>2</sub>O<sub>3</sub> ratio (80) and nickel incorporation (1 wt%) were used to modify HZSM-5 zeolite (SiO<sub>2</sub>/Al<sub>2</sub>O<sub>3</sub> ratio of 30) during bio-oil catalytic cracking at 500 °C in a fluidized bed reactor [89]. The modified HZSM-5 catalysts regeneration were conducted by combusting coke with air at 550 °C for 2 h, the regenerated catalysts maintained similar activities for ten reaction–regeneration cycles. The main reason for the stability of these modified catalysts was due to the homogeneity, moderate acid strength, and low density of acid sites in the catalysts.

Recycle of used catalyst is beneficial to prolong the catalyst life. Reusability of Zn, Ce, and Ni metal doped Al<sub>2</sub>O<sub>3</sub> catalysts was tested for in-situ catalytic upgrading of sunflower stalk derived bio-oil [60]. A five-cycle reusability test of these catalysts showed long-term stability in their performance. Regeneration of spent catalysts was conducted through calcining at 650 °C in air for 0.5 h during the fifth cycle. The possible reason for the catalyst stability was that metal species promoted hydrogen atom migration through C–H activation, catalyzing the oligomerization of intermediates. These intermediates prevented coke formation on the surface of the catalyst.

## 4. Hydrodeoxygenation

Hydrodeoxygenation (HDO) is an effective bio-oil upgrading technique using a variety of heterogeneous catalysts at high hydrogen pressure (7.5–30 MPa) and temperatures (250–450 °C) [91,92]. HDO removes oxygen in bio-oil as H<sub>2</sub>O, CO, and/or CO<sub>2</sub> [93,94]. This results in the production of stable hydrocarbon biofuel with higher energy content. During the bio-oil HDO process, multiple reactions including hydrogenation, hydrogenolysis, hydrodeoxygenation, decarboxylation, decarbonylation, cracking/hydrocracking, and polymerization reactions occurred. An efficient HDO catalyst should effectively remove oxygen with low hydrogen consumption and suppress the coke formation that leads to catalyst deactivation. Various noble and transitional metal catalysts supported on carriers of alumina, silica, titania, zirconia, magnesium oxide, active carbon, and HZSM-5 have been tested on bio-oil and model HDO compounds. The most recent catalysts used for HDO are listed in Table 4.

**Table 4.** Recent advances in heterogeneous catalysts for HDO (hydrodeoxygenation) of bio-oil and model compounds.

| Catalysts   | Feed Stocks  | Temperature (°C) | Pressure (MPa) | Reactor Type           | Main Products   | Product Yield (wt%)            | Product Compositions (Peak Area %) | Coke Yield (wt%) | Findings   | References |
|---|--|------------------|----------------|------------------------|---|--------------------------------|------------------------------------|------------------|--|------------|
| <b>Sulfided catalysts</b>   |  |                  |                |                        |   |                                |                                    |                  |  |            |
| Ni-MoS <sub>2</sub> /ZrO <sub>2</sub> , Sulfided NiMo and CoMo catalysts, Ni/W/TiO <sub>2</sub>   | Phenol, 1-octanol, mallee wood bio-oil, guaiacol   | 150–300          | 5–10           | Packed bed, autoclave  | Cyclohexane, cyclohexene, octane, octane, alkyl phenols | 16–46                          | - <sup>3</sup>                     | 5.7–28.1         | Cl, S and K in bio-oil deactivated catalyst.   | [95–97]    |
| <b>Noble metal catalysts</b>  |  |                  |                |                        |   |                                |                                    |                  |  |            |
| Pt/C  | Miscanthus bio-oil   | 250–350          | 3              | Autoclave              | Heavy oil, light oil                                    | 48.3–83.3 (W <sup>1</sup> )    | -                                  | 3.8–16.1         | Ethanol improved bio-oil quality as a co-reactant.   | [98]       |
| Zn <sup>2+</sup> -Pd/C  | Pine sawdust bio-oil   | 150–350          | 1.38–4.14      | Autoclave              | <b>Hydrocarbons</b>                                     | 40.28–46.72 (OP <sup>2</sup> ) | 0.54–6.06                          | 0.22–0.41        | Zn <sup>2+</sup> and Pd had the synergistic effect for HDO bio-oil upgrading.  | [99]       |
| Ru/MWCNT, Ru/CARE, Ru/Vulcan carbon, Ru/AC, Ru/Graphite, Pt/carbon, Pd/carbon, Pt/HZSM-5, Pt/Mesoporous Beta, Pt/HBeta, Pt/MMZBeta, Pt/Al-MCM-48, Pt/Si-MCM-48, Pt/ZSM-5, Pt/Al <sub>2</sub> O <sub>3</sub> , Pt/SiO <sub>2</sub> , Pt/H-MFI-90 | Oak chips bio-oil, grass bio-oil, eucalyptus bio-oil, benthamii, bio-oil, equine manure bio-oil, guaiacol, cresol, dibenzofuran, 1-octanol | 50–320           | 4–14.5         | Autoclave or fixed-bed | Hydrocarbons  | 0.08–91                        | -                                  | -                | Ru/MWCNT was highly active for producing alkanes and cycloalkanes. Pt/Mesoporous Beta and Pt/HBeta showed higher guaiacol conversions. | [100–103]  |
| Ru/C  | Pine sawdust bio-oil   | 250–300          | 2              | Autoclave              | Esters, ethers  | 42.3–84.6 (W)                  | 40.5                               | 0.2–9.9          | Acids, aldehydes, ketones, phenols and furans contents of upgraded bio-oil decreased significantly.                                    | [104]      |
| <b>Transition metal catalysts</b>   |  |                  |                |                        |   |                                |                                    |                  |  |            |
| Ni/AC, Ni-Fe/AC, Ni-Mo/AC, Ni-Cu/AC, Ni-Co/HZSM-5, Ni-Co/HBeta, Ni-Co/HY, Ni-Co/ZrO <sub>2</sub>  | Prairie cordgrass bio-oil, wood bio-oil  | 250–350          | 3.4–5          | Autoclave              | <b>Hydrocarbons</b>                                     | 17.35–37.0 (OP)                | 16.37–39.42                        | 3.09–8.86        | Ni/AC produced the highest content of gasoline range hydrocarbons. 10Ni10Co/HZSM-5 shows the best performance in bio-oil HDO.          | [92,105]   |
| CoMo/AC, CoMo/γ-Al <sub>2</sub> O <sub>3</sub> , CoMo/HZSM-5, CoMo/MCM-41, Sawdust bio-oil CoMo/SBA-15, Ru/C  |  | 300–350          | 20.7–22.5      | Autoclave              | Heavy oil, light oil                                    | 55.0–66.6 (W)                  | -                                  | <1–10            | CoMo/MCM-41 had better resistance to coke deposition than other CoMo catalysts.  | [106]      |

Table 4. Cont.

| Catalysts  | Feed Stocks  | Temperature (°C) | Pressure (MPa) | Reactor Type                        | Main Products   | Product Yield (wt%) | Product Compositions (Peak Area %) | Coke Yield (wt%) | Findings  | References |
|--|--|------------------|----------------|-------------------------------------|---|---------------------|------------------------------------|------------------|---|------------|
| Raney Ni, nafion/SiO <sub>2</sub> , nano Ni/SiO, Ni/HBeta, Fe/HBeta, NiFe/HBeta, Ni/HZSM-5, Ni/ZSM-5, Co/ZSM-5, Ni/SBA-15, Co/SBA-15, Ni/Al-SBA-15, Co/Al-SBA-15, Ni/Ce-SBA-15, Cu-Ni/TiO <sub>2</sub> , Cu-Ni/ZrO <sub>2</sub> , Cu-Ni/CeO <sub>2</sub>   | Phenol, o-cresol, anisole, dibenzo furan             | 160–340          | 0.7–10         | Autoclave, Fixed-bed                | Hydrocarbons  | 3.1–92.4            | -                                  | -                | Raney Ni was effective for hydrogenation and Nafion/SiO <sub>2</sub> was effective for dehydration. Small nickel particles favored deoxygenation and large particles favored hydrogenation. | [107–113]  |
| Ni/CMK-3, MoNi/γ-Al <sub>2</sub> O <sub>3</sub>  | Pine sawdust bio-oil                                 | 100–230          | 0.1–3          | Autoclave                           | Alcohols, esters  | -                   | 48.21–51.14                        | -                | Hydrogen donors provided hydrogen for in-situ hydrogenation. Mo addition inhibited the formation of NiAl <sub>2</sub> O <sub>4</sub> .  | [114,115]  |
| Co/Al-MCM-41, Ni/Al-MCM-41, NiCo/Al-MCM-41, Cu/C, Fe/C, Pd/C, Pt/C, PdFe/C, Ru/C, Ni@Pd/silica alumina, Ni@Pt/silica alumina, CuRe/SiO <sub>2</sub> , Ni/MCM-41, HZSM-5, Ni/ZrO <sub>2</sub> -SiO <sub>2</sub> , NiCu/ZrO <sub>2</sub> -SiO <sub>2</sub>   | Guaiacol   | 120–450          | 0.1–5          | Fixed-bed, autoclave                | Hydrocarbons  | 0.1–95.4            | -                                  | -                | Co was active in HDO via C–O hydrogenolysis and Ni favored C–C hydrogenolysis. Pd-Fe catalyst was active and selective for HDO. Overlayer catalysts enhanced deoxygenation activity.        | [116–121]  |
| <b>Other catalysts</b>   |  |                  |                |                                     |   |                     |                                    |                  |   |            |
| Ni-NS, Ru-NS, Ni-Al <sub>2</sub> O <sub>3</sub> , Ni/SiO <sub>2</sub> -Al <sub>2</sub> O <sub>3</sub> , Pine wood AC, coconut shell AC, bamboo stem AC, apricot pit AC, peach pit AC, coal AC,   | Pine bio-oil, duckweed bio-oil                       | 300–400          | 4.1–6          | Autoclave                           | Hydrocarbons  | 51.6–98.8 (W)       | 46.37–89.37                        | 5.3–10.1         | NS catalysts showed promising effect for upgrading bio-oils to biofuels.  | [122,123]  |
| CoP/Al <sub>2</sub> O <sub>3</sub> , CoMoP/γ-Al <sub>2</sub> O <sub>3</sub> , MoP/γ-Al <sub>2</sub> O <sub>3</sub> , Ni <sub>2</sub> P/γ-Al <sub>2</sub> O <sub>3</sub> , Ni/γ-Al <sub>2</sub> O <sub>3</sub> , Co/γ-Al <sub>2</sub> O <sub>3</sub> , Ni <sub>2</sub> P/γ-Al <sub>2</sub> O <sub>3</sub> , CoP/γ-Al <sub>2</sub> O <sub>3</sub> , CeZrO <sub>x</sub> | 2-furyl methyl ketone, acetic acid, acetol, furfural | 250–400          | 0.1            | Fixed-bed                           | Methyl cyclopentane, cyclohexane, pyruvaldehyde, 1,2-propylene glycol | 11–100              | -                                  | -                | CoP/Al <sub>2</sub> O <sub>3</sub> had higher selectivity to methyl cyclopentane.   | [124–126]  |
| CoMo/MgO, CoMoP/MgO, Ni-W-P-B, Ni <sub>2</sub> P/γ-Al <sub>2</sub> O <sub>3</sub> , MoP/γ-Al <sub>2</sub> O <sub>3</sub> , Mo <sub>2</sub> C/TiO <sub>2</sub> , MoP/TiO <sub>2</sub> , Mo <sub>2</sub> N/TiO <sub>2</sub> , MoO <sub>3</sub> /TiO <sub>2</sub>   | Phenol, p-cresol, palmitic acid                      | 180–450          | 2.5–5          | Micro-reactor, autoclave, fixed-bed | Benzene, toluene, pentadecane, cyclohexyl-aromatics                   | -                   | 13.23–64.23                        | -                | CoMoP/MgO showed superior activity in phenol HDO.   | [127–130]  |

<sup>1</sup> is total bio-oil yield; <sup>2</sup> is oil phase yield; <sup>3</sup> not available.

#### 4.1. Catalysts Used in Bio-Oil HDO

##### 4.1.1. Sulfided Catalysts

Sulfided catalysts including mixed sulfides of (Co, Ni) and (Mo, W) dispersed on  $\gamma$ -Al<sub>2</sub>O<sub>3</sub> or MgO have been used for bio-oil HDO due to the good catalytic performance [131,132]. Sulfided CoMo/ $\gamma$ -Al<sub>2</sub>O<sub>3</sub> and NiMo/ $\gamma$ -Al<sub>2</sub>O<sub>3</sub> catalysts were used for wood-derived bio-oil HDO upgrading [133]. The results indicated that CoMo/ $\gamma$ -Al<sub>2</sub>O<sub>3</sub> showed higher selectivity to diesel-like products and higher activity for removal of gaseous intermediates (CO<sub>x</sub>) by hydrogenation than NiMo/ $\gamma$ -Al<sub>2</sub>O<sub>3</sub>. The active sites that exhibited Lewis acid character on sulfided catalysts were sulphur anion vacancies (coordinately unsaturated sites), and located at the edges of MoS<sub>2</sub> nanoclusters [134]. Compared with NiMo/ $\gamma$ -Al<sub>2</sub>O<sub>3</sub> catalyst, NiW/ $\gamma$ -Al<sub>2</sub>O<sub>3</sub> catalyst presented a higher isomerization activity leading to higher phenol conversion in phenol HDO [134]. In sulfided NiW catalysts, WS<sub>2</sub> was the HDO active phase while Ni was used as the promoter. Phosphorus (P) doping has been used to improve the activity of sulfide catalysts, and CoMoP/MgO catalyst showed higher activity for phenol HDO than CoMo/MgO [130]. The activity-promoting effects of P was due to the increase in Mo dispersion, stacking of MoS<sub>2</sub> crystallites and formation of new Lewis and Brønsted acid sites on the catalyst surface.

Sulfided catalysts are not very desirable for bio-oil HDO due to the addition of sulfur-containing compounds. They can result in the contamination of biofuel products and increase upgrading cost. Besides, alumina is unstable under hydrothermal conditions, and it can partially transform into boehmite in the presence of water vapor at reaction temperature (140–380 °C) [107]. Finally, Al<sub>2</sub>O<sub>3</sub> support shows a high tendency for polymerization reactions due to the high acidity resulting in coke deposition [93].

##### 4.1.2. Noble Metal Catalysts

Noble metal (Rh, Pt, Pd, and Ru) catalysts showed excellent bio-oil HDO catalytic performance. These catalysts do not require the consumption of environmentally unfriendly sulfur compounds. These metal catalysts are active at low temperatures, and this could possibly prevent thermal reactions leading to coke formation and deactivation. The effectiveness of noble metal catalysts was affected by the types of biomass and noble metals. During HDO of fast-pyrolysis bio-oils from several feedstocks (switchgrass, eucalyptus benthamii, and equine manure) using Pt/C, Ru/C, and Pd/C catalysts, switchgrass bio-oil over Pt/C showed the best hydrogen consumption and deoxygenation efficiency [25]. A variety of heterogeneous noble-metal catalysts (Ru/C, Ru/TiO<sub>2</sub>, Ru/Al<sub>2</sub>O<sub>3</sub>, Pt/C, and Pd/C) were screened for the upgrading of beech wood fast pyrolysis oil [135]. Among the tested catalysts, Ru/C catalyst was found to be the most effective catalyst with respect to oil yield (up to 60 wt%) and deoxygenation level (up to 90 wt%). HDO of pinewood derived bio-oil using monometallic and bimetallic noble metal (Rh, Pd, Pt) catalysts supported on ZrO<sub>2</sub> showed Pd/ZrO<sub>2</sub> produced the highest activity followed by Rh/ZrO<sub>2</sub> [136]. This was due to the higher sulfur (present in bio-oil) tolerance of Pd/ZrO<sub>2</sub> than other metal catalysts.

The support properties including pore sizes, acidity, and surface areas have a significant influence on noble metal catalyst activity. Pt/ZSM-5 showed much higher deoxygenation ability than Pt/Al<sub>2</sub>O<sub>3</sub> during HDO of pyrolysis bio-oil [101]. This was attributed to the mesoporous structure and high acidity of Pt/ZSM-5. Pt catalysts supported over carriers such as HZSM-5, Mesoporous Beta, HBeta, MMZBeta, Al-MCM-48, and Si-MCM-48 were tested for HDO of guaiacol in a batch-type reactor at 4 MPa and 250 °C [102]. This study indicated that Pt/Mesoporous Beta and Pt/HBeta catalysts showed higher guaiacol conversions due to the large pores and strong acid sites of the catalysts. Five carbon materials including multi-walled carbon nanotubes (MWCNT), carbon aerogel (CARF), carbonblack (Vulcan carbon), activated carbon (AC), and graphite were used as supports for Ru catalysts for HDO of oak chips pyrolysis oil [100]. The results showed that Ru/MWCNT exhibited the highest deoxygenation activity as a result of the high Ru surface area and external surface area of the MWCNTs.

The availability and high cost of noble metals are the main challenges for the application of noble metal catalysts. Besides, noble metal catalysts show a rather low resistance towards poisoning by low levels of elements such as iron or sulfur in bio-oil when compared to sulfided catalysts [129].

#### 4.1.3. Transition Metal Catalysts

Transition metal catalysts showed good catalytic performance for bio-oil upgrading. They can be used as a potential alternative for precious metal and sulfided catalysts due to the high activity and low cost. For instance, non-sulfided catalysts including MoNi/ $\gamma$ -Al<sub>2</sub>O<sub>3</sub>, NiCu/ $\delta$ -Al<sub>2</sub>O<sub>3</sub>, and NiFe/ $\gamma$ -Al<sub>2</sub>O<sub>3</sub> have attracted much attention because of their good catalytic activity for HDO of pyrolysis oil [115–138]. MoNi/ $\gamma$ -Al<sub>2</sub>O<sub>3</sub> considerably improved properties of pine sawdust bio-oil including hydrogen content and the acidity [115]. The addition of Mo as a promoter benefited nickel species uniformity and inhibited NiAl<sub>2</sub>O<sub>4</sub> spinel formation in MoNi/ $\gamma$ -Al<sub>2</sub>O<sub>3</sub> catalyst. Bimetallic Ni-Cu/ $\delta$ -Al<sub>2</sub>O<sub>3</sub> catalysts were more active and outperformed monometallic Ni/ $\delta$ -Al<sub>2</sub>O<sub>3</sub> or Cu/ $\delta$ -Al<sub>2</sub>O<sub>3</sub> for the HDO of fast pyrolysis oil [137]. This was due to the smaller size and increased number of active Ni<sub>x</sub>Cu<sub>1-x</sub> clusters in the catalyst. NiFe/ $\gamma$ -Al<sub>2</sub>O<sub>3</sub> improved the heating value of straw bio-oil from 37.8 MJ/kg to 43.9 MJ/kg after bio-oil HDO. This was due to the formation of NiFe alloy in the NiFe/ $\gamma$ -Al<sub>2</sub>O<sub>3</sub> catalysts [138]. The major reaction pathway was the cleavage of C–O rather than C–C during the bio-oil HDO process. Fe/SiO<sub>2</sub> was an active and selective catalyst for HDO upgrading of guaiacol to produce aromatic hydrocarbons, and it exhibited a good selectivity for BT (benzene, toluene) production [139].

Four inexpensive transitional metal catalysts including Ni/AC, Ni-Fe/AC, Ni-Mo/AC, and Ni-Cu/AC were investigated for HDO of prairie cordgrass bio-oil [92]. The results indicated that Ni/AC catalysts produced upgraded bio-oil with the highest content of gasoline range hydrocarbons (32.63%). This was due to hydrogenation reactions promoted by Ni. Ni-Mo/AC generated the upgraded bio-oil with the highest content of gasoline blending alkyl-phenols at 38.41%. Ni-Mo/AC catalysts inhibited the C–C breaking and promoted C–O activation, which led to a higher degree of deoxygenation (66.02%) than Ni/AC (63.60%). Bifunctional metal/acid catalysts including Ni/HBeta, Fe/HBeta, and NiFe/HBeta were used for HDO of a simulated phenolic bio-oil consisting of phenol, o-cresol, and guaiacol [108]. The results indicated that bimetallic NiFe/HBeta catalyst showed higher HDO activity when compared to monometallic Ni/HBeta and Fe/HBeta. This is due to the synergistic effect between the two metals. NiFe/HBeta catalysts converted phenolic compounds to oxygen-free products via hydrogenation and hydrogenolysis reactions.

#### 4.1.4. Other Catalysts

Amorphous catalysts exhibited excellent activity and good selectivity during bio-oil HDO reactions because of their unique isotropic and high concentration of coordinative unsaturated sites. Boron (B) amorphous catalysts such as Co-Mo-B and Co-Ni-Mo-B catalysts exhibited high catalytic activity in HDO of bio-oil model compounds including phenol, benzaldehyde, and acetophenone [140,141]. It was attributed to sufficient supply of free hydrogen, decreased catalyst particle size and high content of Mo<sup>4+</sup> Brønsted acid sites on the catalyst surface. Ni-W-P-B amorphous catalyst also exhibited high HDO and dehydrogenation activities during the HDO of *p*-cresol due to the high Ni<sup>0</sup>, P<sup>0</sup>, and P<sup>n+</sup> contents on the catalyst surface [127]. The deoxygenation degree was 100% with a toluene selectivity of 5.1% at 225 °C.

Carbides, nitrides, and phosphides catalysts have drawn considerable interest due to their potential use for bio-oil HDO processes. Carbide (C) catalysts including NiMoC/SiO<sub>2</sub> were highly active and stable catalysts for HDO of model bio-oil compounds including ethyl benzoate, acetone, and acetaldehyde. This was attributed to the acid sites on the surface of the NiMo carbide catalysts [142]. Nitride (N) catalysts of Mo<sub>2</sub>N were evaluated for HDO of guaiacol in a batch autoclave at 300 °C and 5 MPa [143]. Mo<sub>2</sub>N catalyst prepared with flowing ammonia showed the highest activity for guaiacol conversion due to  $\gamma$ -Mo<sub>2</sub>N phase and high N/Mo atomic ratio present in the catalyst. Phosphides (P) catalysts such as CoP/ $\gamma$ -Al<sub>2</sub>O<sub>3</sub> showed higher activity during HDO of 2-furyl methyl ketone

(FMK) [124]. The complete conversion of FMK into methyl cyclopentane at 400 °C was achieved over 10 wt% CoP/Al<sub>2</sub>O<sub>3</sub> catalyst due to its high acidity value, adequate surface area, and pore size. Nickel phosphide catalyst Ni<sub>2</sub>P/SiO<sub>2</sub> was compared with traditional catalysts (Ni/SiO<sub>2</sub>, Pd/C, ZSM-5, SiO<sub>2</sub>-Al<sub>2</sub>O<sub>3</sub>, and FCC) for direct catalytic upgrading of cedar chips pyrolysis bio-oil [144]. The results indicated that the deoxygenation activity of Ni<sub>2</sub>P/SiO<sub>2</sub> was higher than that of conventional catalysts including Ni/SiO<sub>2</sub>, Pd/C, ZSM-5, SiO<sub>2</sub>-Al<sub>2</sub>O<sub>3</sub>, and FCC.

Silica nanosprings (NS) with large surface-to-volume ratios are promising silica supports. NS supported nickel and ruthenium catalysts (Ni/NS and Ru/NS) resulted in higher activity during HDO of phenol and bio-oil compared to conventional Ni/Al<sub>2</sub>O<sub>3</sub> and Ni/gel silica catalysts. This results from lower volume mesoporous pores and better metal dispersion in NS supported catalysts [122].

Activated carbon alone can be used as an effective catalyst for deoxygenation and denitrogenation of bio-oil. This is attributed to AC mesopore properties including an affinity for heavy hydrocarbon compounds and an excellent ability to restrict coke formation. Five commercial ACs (pine wood AC, coconut shell AC, bamboo stem AC, apricot pit AC, peach pit AC, and coal AC) were tested for catalytic upgrading of crude bio-oil produced from the hydrothermal liquefaction of duckweed [123]. The results indicated that ACs exhibited similar deoxygenation and denitrogenation activity compared to Ru/C. Bamboo stem AC produced upgraded bio-oil with the highest yield (76.3 wt%) and energy density (44.1 MJ/kg).

#### 4.2. Catalyst Deactivation in Bio-Oil HDO

The main problem for the bio-oil HDO process is formation of coke resulting from the thermal instability of bio-oil. This leads to catalyst deactivation and decreased catalyst lifetime. The deactivation behavior of the catalyst in bio-oil HDO is discussed in the study of Lee et al. [145]. Coking is principally due to the deposition of polyaromatic species through polymerization and polycondensation reactions on the catalyst's surface [146]. The coke blocks the catalyst pores and masks the active sites on the surface. The coke formation during HDO of mallee wood bio-oil over sulfided NiMo and CoMo catalysts indicated severe coke formation on catalysts due to polymerization of the heavy fraction in the upgraded bio-oil. This was accompanied by the formation of large aromatic ring structures [96]. Deactivation mechanisms of Ru/C and Pt/C catalysts during the HDO conversion of guaiacol confirmed that coking due to the polyaromatic deposits, particularly condensed ring series compounds, were the main cause of catalyst deactivation [147].

Coking formation is related to the acidity of the catalysts, and coking increases with increased catalyst acidity. Alumina acidic support was deactivated faster than inert supports such as SiO<sub>2</sub> due to its relatively high acidity and strong interaction with the coke precursors [117,148]. A high density of Brønsted acid sites resulted in condensation of precursors adsorbed on adjacent sites and faster coke formation [149]. Acidity of the catalyst is also necessary for catalyst activity. Therefore, similar to catalytic cracking catalysts, a balance between catalyst activity and deactivation should be optimized to design the optimal strength of catalyst acidity for bio-oil HDO.

Coking deposition also strongly depends on the types of feedstock. Unsaturated hydrocarbons such as alkenes and aromatics have a higher tendency for coking due to the increased interactions between the C=C bond and aromatic rings with the active catalysts sites [146]. Oxygenated compounds with two or more oxygen atoms showed a stronger potential for carbon formation by polymerization reactions [150].

#### 4.3. Reducing Catalyst Deactivation in Bio-Oil HDO

A big challenge is catalyst deactivation caused by catalyst acidity and support instability induced by water at high temperature. Using catalyst supports containing lower acidity and higher stability is an effective method to retard coke formation. Compared to acidic supports (Al<sub>2</sub>O<sub>3</sub>), neutral activated carbon (AC) or silica (SiO<sub>2</sub>) can be utilized as alternative catalyst supports [151]. The Lewis acidic sites

on alumina-supported CoMo catalysts resulted in large coke formation during HDO reaction, while the HDO reaction over AC supported CoMo catalysts showed almost no coking reactions [152].

Optimizing bio-oil HDO operation conditions reduces coke formation. Increasing hydrogen pressure saturates the carbon precursors, and was beneficial for decreasing the coke formation in reference [153]. Hydrogen can react with and stabilize the reactive fragments before they undergo polymerization and condensation reactions that result in coke formation. Bio-oil HDO reaction temperature has a significant influence on coke formation. Increased reaction temperature will generally result in increased carbon formation on catalysts. This is attributed to the promotion of polymerization and polycondensation reactions [99]. Therefore, moderate temperature should be used to reduce coke formation.

Integrated bio-oil upgrading processes can reduce coking formation and inhibit bio-oil repolymerization. A two-stage bio-oil HDO process (low-temperature (170 °C) and high-temperature (400 °C)) using Ru/C and sulfided CoMo/Al<sub>2</sub>O<sub>3</sub> catalyst in a continuous process was proposed by Elliott et al. [154]. It was effective in avoiding excessive coking due to the depressed polymerization and stabilization of pretreated bio-oil during the low-temperature HDO step. The two-step bio-oil upgrading (including esterification and HDO) produced more stable bio-oil with lower coking tendency and less large aromatic ring systems than the one step HDO bio-oil [155]. The low coke yield was due to the reactive oxygen-containing functional groups in the raw bio-oil which were effectively stabilized through esterification.

Co-processing bio-oil with hydrogen donor solvents, waste lubricating oil, and sugars can decrease the undesirable carbon deposition on catalysts. The effects of hydrogen donor solvents used during bio-oil HDO and their roles in decreasing catalysts deactivation are discussed by Lee et al. [145]. The roles of hydrogen donor solvents include reducing mass-transfer limitations, promoting cracking and hydrogenation reactions, diluting lignin, and decreasing polymerization at high reaction temperatures [156]. Studies have been conducted for upgrading bio-oils using hydrogen donor solvents to reduce coke formation by enhancing the stability of the bio-oil to temperature effects. Ethanol, acetone, ether, 1-butanol, and tetralin were effective in retarding formation of coke precursors and also extracting the coke precursors from the catalyst pores. Coke formation was reduced over Ru/C, Pt/C, Rh/C, and sulfided Co–Mo–P catalysts during bio-oil HDO processes [104,156,157]. HDO upgrading of bio-oil using supercritical 1-butanol over Ru/C catalyst [125] limited carbon deposition to only 0.2 wt% compared to 9.9 wt% without a solvent. The 1-butanol serves as the reaction medium and reactant, facilitating hydrogen dissolution, protecting the catalyst, and improving the upgraded bio-oil product properties (oxygen content and HHV) during the bio-oil HDO process. Reaction pathways including esterification, etherification, acetalization, hydrogenation, and hydrodeoxygenation have been proposed. Co-HDO bio-oil and used engine oil (UEO) over Pt/C and Rh/C catalysts were investigated by Wang Feng and his colleagues [153,158]. UEO suppressed coke formation was confirmed in the bio-oil co-HDO process. This can be attributed to dispersing and clearing agents in the UEO which played an important role in the control of coke formation. Sugars have the tendency to reduce coke formation. The role of sugars on coke formation was investigated by adding levoglucosan into the bio-oil HDO process over sulfided NiMo catalyst [96]. The results indicated that adding levoglucosan to bio-oil over NiMo catalyst slightly decreased the coke yield at 300 °C. The NiMo catalyst prevented the formation of additional large aromatic ring systems when the levoglucosan was added.

#### 4.4. Catalyst Regeneration and Recycle in Bio-Oil HDO

In order to reduce operation cost, deactivated HDO catalysts need to be regenerated or recycled. The catalyst regeneration is generally done by coke oxidation in an air stream at mild temperatures (350–600 °C). Catalyst regeneration generally consists of three main steps: (1) spent catalysts with adsorbed organic species are washed by solvents and dried; (2) dried catalysts are calcined in an oxygen-containing gas, such as air, to remove coke; and (3) the calcined catalysts are reduced in a hydrogen-containing gas.

Used Pt/H-MFI-90 catalysts with coke deposition were washed with ethanol and methanol, calcined in air at 400 °C for 10 h and reduced in a continuous hydrogen flow [103]. The regeneration experiments for HDO of guaiacol and 1-octanol showed that the catalytic conversion of guaiacol and 1-octanol over recovered Pt/H-MFI-90 catalysts was partly restored, and the recovered catalyst deactivated faster than the fresh catalyst. Spent CoMo/MCM-41 catalyst for HDO of fast pyrolysis oil was regenerated in air at 600 °C for 2 h [106]. Although the regenerated catalyst produced similar bio-oil yields to the fresh catalyst, the hydrogenation activity of the regenerated catalyst decreased in comparison with fresh catalyst. Spent NiFe/HBeta catalyst used for HDO of simulated phenolic bio-oil was regenerated by washing with acetone and water, drying in ambient air at 110 °C for 8 h and calcining in air at 550 °C [108]. Considerable decrease in conversion of phenolic compounds and selectivity of oxygen-free products over regenerated NiFe/HBeta catalyst was observed by the fourth recycle run. This was caused by increased loss of metal active sites and the reduction of catalyst surface area and pore volume. Regeneration of Pt/ $\gamma$ -Al<sub>2</sub>O<sub>3</sub>, Pt/SiO<sub>2</sub>, and Pt/Na-B catalysts was conducted in air at 350 °C for m-cresol HDO. The recovered catalysts obtained the same activity and selectivity toward toluene in the second cycle compared to the first cycle [149]. This was due to the recovered metallic sites and a high fraction of acid sites in the regenerated catalysts.

The used HDO catalysts containing coke can also be recycled to extend catalyst lifetime. For AC supported catalyst, it is difficult to remove catalyst coke by a simple air combustion method because the support is easily burned. Recycling of the used AC supported catalyst is more feasible to improve catalyst life. The reused Ru/C catalyst was washed with ethanol. The recycled Ru/C showed that the catalyst selectivity toward desired products (alcohols/ethers) decreased gradually with the number of catalyst recycle times due to coke deposition [159]. The recyclability of used Ni-Cu/ZrO<sub>2</sub>-SiO<sub>2</sub> using ethanol washing was evaluated for guaiacol HDO at 300 °C and 5.0 MPa [121]. The results indicated that guaiacol conversion and benzene selectivity decreased significantly by the fourth recycle due to the formation of coke and residual polymers deposited on the catalyst surface.

## 5. Summary and Outlook

Biomass has great potential for conversion to transportation fuels through fast pyrolysis and subsequent upgrading processes. Catalytic cracking and HDO are two of the most promising chemical methods to upgrade bio-oils into liquid biofuels. Progress has been made in applications of heterogeneous catalysts during catalytic cracking and HDO. However, catalyst deactivation due to coking created from polymerization and polycondensation reactions still remains a challenge for bio-oil catalytic cracking and HDO processes. Different techniques including metal incorporation, co-processing high C/H ratio feedstocks, using different catalyst supports, as well as modifying operation parameters and process integrations were used to retard coking of catalysts during bio-oil upgrading processes. Air combustion is commonly used to remove coke deposited on catalysts, but this catalyst regeneration method cannot recover the catalyst activity completely. New catalyst regeneration techniques including using diluents like nitrogen and steam need to be developed. Available catalysts need further development to have higher selective activity, long-term stability, and easier regeneration properties without significant loss of activity before testing can be completed in an industrial scale biofuel production plant. In order to exploit appropriate heterogeneous catalysts to produce gasoline or diesel grade biofuel at a commercial scale, some suggestions for future research include:

1. Improve understanding of catalyst deactivation and regeneration mechanisms during bio-oil upgrading processes.
2. Develop effective catalysts with higher stability and better regeneration properties.
3. Integrate upgrading approaches of bio-oil catalytic cracking and/or hydrodeoxygenation with petroleum refining technologies to improve bio-oil upgrading efficiency.
4. Explore new biomass resources or genetically engineered biomass to improve the yield and quality of bio-oils produced.

**Acknowledgments:** This work was supported by U.S. Department of Energy (Award No. SA0900160) and Department of Transportation (Award No. SA0700149) through the North Central Center of Sun Grant Initiative. South Dakota Innovation Partner (Grant No. SA1600799) also partially supported this work.

**Author Contributions:** All the authors contributed in a team work to the review paper. Shouyun Cheng and Lin Wei wrote different parts of the manuscript. Lin Wei and Xianhui Zhao revised and proof read the original version of the paper. James Julson revised and proof read this version of the paper.

**Conflicts of Interest:** The authors declare no conflict of interest.

## References

1. Mohr, S.H.; Wang, J.; Ellem, G.; Ward, J.; Giurco, D. Projection of world fossil fuels by country. *Fuel* **2015**, *141*, 120–135. [[CrossRef](#)]
2. Zhang, H.; Carlson, T.R.; Xiao, R.; Huber, G.W. Catalytic fast pyrolysis of wood and alcohol mixtures in a fluidized bed reactor. *Green Chem.* **2012**, *14*, 98–110. [[CrossRef](#)]
3. Jahirul, M.I.; Rasul, M.G.; Chowdhury, A.A.; Ashwath, N. Biofuels production through biomass pyrolysis—A technological review. *Energies* **2012**, *5*, 4952–5001. [[CrossRef](#)]
4. Masnadi, M.S.; Grace, J.R.; Bi, X.T.; Lim, C.J.; Ellis, N. From fossil fuels towards renewables: Inhibitory and catalytic effects on carbon thermochemical conversion during co-gasification of biomass with fossil fuels. *Appl. Energy* **2015**, *140*, 196–209. [[CrossRef](#)]
5. Mohan, D.; Pittman, C.U.; Steele, P.H. Pyrolysis of wood/biomass for bio-oil: A critical review. *Energy Fuels* **2006**, *20*, 848–889. [[CrossRef](#)]
6. Chhiti, Y.; Kemiha, M. Thermal conversion of biomass, pyrolysis and gasification: A review. *Int. J. Eng. Sci.* **2013**, *2*, 75–85.
7. Gorgens, J.F.; Carrier, M.; Garcia-Aparicio, M.P. Biomass conversion to bioenergy products. In *Bioenergy from Wood: Sustainable Production in the Tropics*; Seifert, T., Ed.; Springer: London, UK, 2013; pp. 158–159.
8. Goyal, H.B.; Seal, D.; Saxena, R.C. Bio-fuels from thermochemical conversion of renewable resources: A review. *Renew. Sustain. Energy Rev.* **2008**, *12*, 504–517. [[CrossRef](#)]
9. Vamvuka, D. Bio-oil, solid and gaseous biofuels from biomass pyrolysis processes—An overview. *Int. J. Energy Res.* **2011**, *35*, 835–862. [[CrossRef](#)]
10. Cao, Y.; Pawłowski, A. Sewage sludge-to-energy approaches based on anaerobic digestion and pyrolysis: Brief overview and energy efficiency assessment. *Renew. Sustain. Energy Rev.* **2012**, *16*, 1657–1665. [[CrossRef](#)]
11. Lu, Q.; Li, W.Z.; Zhu, X.F. Overview of fuel properties of biomass fast pyrolysis oils. *Energy Convers. Manag.* **2009**, *50*, 1376–1383. [[CrossRef](#)]
12. Heo, H.S.; Park, H.J.; Park, Y.K.; Ryu, C.; Suh, D.J.; Suh, Y.W.; Yim, J.W.; Kim, S.S. Bio-oil production from fast pyrolysis of waste furniture sawdust in a fluidized bed. *Bioresour. Technol.* **2010**, *101*, S91–S96. [[CrossRef](#)] [[PubMed](#)]
13. Kim, T.S.; Kim, J.Y.; Kim, K.H.; Lee, S.; Choi, D.; Choi, I.G.; Choi, J.W. The effect of storage duration on bio-oil properties. *J. Anal. Appl. Pyrolysis* **2012**, *95*, 118–125. [[CrossRef](#)]
14. Xu, J.; Jiang, J.; Sun, Y.; Lu, Y. Bio-oil upgrading by means of ethyl ester production in reactive distillation to remove water and to improve storage and fuel characteristics. *Biomass Bioenergy* **2008**, *32*, 1056–1061.
15. Oasmaa, A.; Kuoppala, E. Fast pyrolysis of forestry residue. 3. Storage stability of liquid fuel. *Energy Fuels* **2003**, *17*, 1075–1084. [[CrossRef](#)]
16. Kim, S.J.; Jung, S.H.; Kim, J.S. Fast pyrolysis of palm kernel shells: Influence of operation parameters on the bio-oil yield and the yield of phenol and phenolic compounds. *Bioresour. Technol.* **2010**, *101*, 9294–9300. [[CrossRef](#)] [[PubMed](#)]
17. Zheng, J.-L. Bio-oil from fast pyrolysis of rice husk: Yields and related properties and improvement of the pyrolysis system. *J. Anal. Appl. Pyrolysis* **2007**, *80*, 30–35.
18. DeSisto, W.J.; Hill, N.; Beis, S.H.; Mukkamala, S.; Joseph, J.; Baker, C.; Ong, T.H.; Stemmler, E.A.; Wheeler, M.C.; Frederick, B.G.; et al. Fast pyrolysis of pine sawdust in a fluidized-bed reactor. *Energy Fuels* **2010**, *24*, 2642–2651. [[CrossRef](#)]
19. Greenhalf, C.E.; Nowakowski, D.J.; Harms, A.B.; Titiloye, J.O.; Bridgwater, A.V. A comparative study of straw, perennial grasses and hardwoods in terms of fast pyrolysis products. *Fuel* **2013**, *108*, 216–230. [[CrossRef](#)]

20. Trinh, T.N.; Jensen, P.A.; Dam-Johansen, K.; Knudsen, N.O.; Sørensen, H.R.; Hvilsted, S. Comparison of lignin, macroalgae, wood, and straw fast pyrolysis. *Energy Fuels* **2013**, *27*, 1399–1409. [[CrossRef](#)]
21. Yanik, J.; Stahl, R.; Troeger, N.; Sinag, A. Pyrolysis of algal biomass. *J. Anal. Appl. Pyrolysis* **2013**, *103*, 134–141. [[CrossRef](#)]
22. Abdullah, N.; Sulaiman, F.; Gerhauser, H. Characterisation of oil palm empty fruit bunches for fuel application. *J. Phys. Sci.* **2011**, *22*, 1–24.
23. Ryu, Y.; Lee, Y.; Nam, J. Performance and emission characteristics of additives-enhanced heavy fuel oil in large two-stroke marine diesel engine. *Fuel* **2016**, *182*, 850–856. [[CrossRef](#)]
24. Park, J.; Jang, J.H.; Park, S. Effect of fuel temperature on heavy fuel oil spray characteristics in a common-rail fuel injection system for marine engines. *Ocean Eng.* **2015**, *104*, 580–589. [[CrossRef](#)]
25. Elkasabi, Y.; Mullen, C.A.; Pighinelli, A.L.; Boateng, A.A. Hydrodeoxygenation of fast-pyrolysis bio-oils from various feedstocks using carbon-supported catalysts. *Fuel Process. Technol.* **2014**, *123*, 11–18. [[CrossRef](#)]
26. Zhou, M.; Xiao, G.; Wang, K.; Jiang, J. Catalytic conversion of aqueous fraction of bio-oil to alcohols over CNT-supported catalysts. *Fuel* **2016**, *180*, 749–758. [[CrossRef](#)]
27. Wang, S.; Cai, Q.; Chen, J.; Zhang, L.; Zhu, L.; Luo, Z. Co-cracking of bio-oil model compound mixtures and ethanol over different metal oxide-modified HZSM-5 catalysts. *Fuel* **2015**, *160*, 534–543. [[CrossRef](#)]
28. Luo, G.; Resende, F.L. In-situ and ex-situ upgrading of pyrolysis vapors from beetle-killed trees. *Fuel* **2016**, *166*, 367–375. [[CrossRef](#)]
29. Gamliel, D.P.; Du, S.; Bollas, G.M.; Valla, J.A. Investigation of in situ and ex situ catalytic pyrolysis of miscanthus × giganteus using a PyGC–MS microsystem and comparison with a bench-scale spouted-bed reactor. *Bioresour. Technol.* **2015**, *191*, 187–196. [[CrossRef](#)] [[PubMed](#)]
30. Huang, Y.; Wei, L.; Crandall, Z.; Julson, J.; Gu, Z. Combining Mo–Cu/HZSM-5 with a two-stage catalytic pyrolysis system for pine sawdust thermal conversion. *Fuel* **2015**, *150*, 656–663. [[CrossRef](#)]
31. Heo, H.S.; Park, H.J.; Dong, J.I.; Park, S.H.; Kim, S.; Suh, D.J.; Suhd, Y.W.; Kim, S.S.; Park, Y.K. Fast pyrolysis of rice husk under different reaction conditions. *J. Ind. Eng. Chem.* **2010**, *16*, 27–31. [[CrossRef](#)]
32. Mullen, C.A.; Boateng, A.A.; Goldberg, N.M.; Lima, I.M.; Laird, D.A.; Hicks, K.B. Bio-oil and bio-char production from corn cobs and stover by fast pyrolysis. *Biomass Bioenergy* **2010**, *34*, 67–74. [[CrossRef](#)]
33. Ren, S.; Ye, X.P.; Borole, A.P.; Kim, P.; Labbé, N. Analysis of switchgrass-derived bio-oil and associated aqueous phase generated in a semi-pilot scale auger pyrolyzer. *J. Anal. Appl. Pyrolysis* **2016**, *119*, 97–103. [[CrossRef](#)]
34. Obeid, W.; Salmon, E.; Lewan, M.D.; Hatcher, P.G. Hydrous pyrolysis of Scenedesmus algae and algaenan-like residue. *Org. Geochem.* **2015**, *85*, 89–101. [[CrossRef](#)]
35. Venderbosch, R.H.; Prins, W. Fast pyrolysis technology development. *Biofuels Bioprod. Biorefin.* **2010**, *4*, 178–208. [[CrossRef](#)]
36. Oasmaa, A.; Meier, D. Norms and standards for fast pyrolysis liquids: 1. Round robin test. *J. Anal. Appl. Pyrolysis* **2005**, *73*, 323–334. [[CrossRef](#)]
37. Fan, Y.; Cai, Y.; Li, X.; Yu, N.; Yin, H. Catalytic upgrading of pyrolytic vapors from the vacuum pyrolysis of rape straw over nanocrystalline HZSM-5 zeolite in a two-stage fixed-bed reactor. *J. Anal. Appl. Pyrolysis* **2014**, *108*, 185–195. [[CrossRef](#)]
38. Murata, K.; Liu, Y.; Inaba, M.; Takahara, I. Catalytic fast pyrolysis of jatropha wastes. *J. Anal. Appl. Pyrolysis* **2012**, *94*, 75–82. [[CrossRef](#)]
39. Cheng, S.; Wei, L.; Zhao, X.; Kadis, E.; Julson, J. Conversion of Prairie Cordgrass to Hydrocarbon Biofuel over Co-Mo/HZSM-5 Using a Two-Stage Reactor System. *Energy Technol.* **2016**, *4*, 706–713. [[CrossRef](#)]
40. Cheng, S.; Wei, L.; Zhao, X.; Huang, Y.; Raynie, D.; Qiu, C.; Kiratu, J.; Yu, Y. Directly catalytic upgrading bio-oil vapor produced by prairie cordgrass pyrolysis over Ni/HZSM-5 using a two stage reactor. *AIMS Energy* **2015**, *3*, 227–240.
41. Cheng, S.; Wei, L.; Zhao, X. Development of a bifunctional Ni/HZSM-5 catalyst for converting prairie cordgrass to hydrocarbon biofuel. *Energy Sourc. Part A* **2016**, *38*, 2433–2437. [[CrossRef](#)]
42. Cai, Y.; Fan, Y.; Li, X.; Chen, L.; Wang, J. Preparation of refined bio-oil by catalytic transformation of vapors derived from vacuum pyrolysis of rape straw over modified HZSM-5. *Energy* **2016**, *102*, 95–105. [[CrossRef](#)]
43. Veses, A.; Puértolas, B.; Callén, M.S.; García, T. Catalytic upgrading of biomass derived pyrolysis vapors over metal-loaded ZSM-5 zeolites: Effect of different metal cations on the bio-oil final properties. *Microporous Mesoporous Mater.* **2015**, *209*, 189–196. [[CrossRef](#)]

44. Widayatno, W.B.; Guan, G.; Rizkiana, J.; Du, X.; Hao, X.; Zhang, Z.; Abudula, A. Selective catalytic conversion of bio-oil over high-silica zeolites. *Bioresour. Technol.* **2015**, *179*, 518–523. [[CrossRef](#)] [[PubMed](#)]
45. Zhao, X.; Wei, L.; Cheng, S.; Huang, Y.; Yu, Y.; Julson, J. Catalytic cracking of camelina oil for hydrocarbon biofuel over ZSM-5-Zn catalyst. *Fuel Process. Technol.* **2015**, *139*, 117–126. [[CrossRef](#)]
46. Zhao, X.; Wei, L.; Cheng, S.; Cao, Y.; Julson, J.; Gu, Z. Catalytic cracking of carinata oil for hydrocarbon biofuel over fresh and regenerated Zn/Na-ZSM-5. *Appl. Catal. A* **2015**, *507*, 44–55. [[CrossRef](#)]
47. Biswas, S.; Sharma, D.K. Effect of different catalysts on the cracking of Jatropha oil. *J. Anal. Appl. Pyrolysis* **2014**, *110*, 346–352. [[CrossRef](#)]
48. Wang, L.; Lei, H.; Bu, Q.; Ren, S.; Wei, Y.; Zhu, L.; Zhang, X.; Liu, Y.; Yadavalli, G.; Lee, J.; Chen, S.; Tang, J. Aromatic hydrocarbons production from ex situ catalysis of pyrolysis vapor over Zinc modified ZSM-5 in a packed-bed catalysis coupled with microwave pyrolysis reactor. *Fuel* **2014**, *129*, 78–85. [[CrossRef](#)]
49. Mihalcik, D.J.; Mullen, C.A.; Boateng, A.A. Screening acidic zeolites for catalytic fast pyrolysis of biomass and its components. *J. Anal. Appl. Pyrolysis* **2011**, *92*, 224–232. [[CrossRef](#)]
50. Widayatno, W.B.; Guan, G.; Rizkiana, J.; Yang, J.; Hao, X.; Tsutsumi, A.; Abudula, A. Upgrading of bio-oil from biomass pyrolysis over Cu-modified  $\beta$ -zeolite catalyst with high selectivity and stability. *Appl. Catal. B* **2016**, *186*, 166–172. [[CrossRef](#)]
51. French, R.; Czernik, S. Catalytic pyrolysis of biomass for biofuels production. *Fuel Process. Technol.* **2010**, *91*, 25–32. [[CrossRef](#)]
52. Liu, S.; Xie, Q.; Zhang, B.; Cheng, Y.; Liu, Y.; Chen, P.; Ruan, R. Fast microwave-assisted catalytic co-pyrolysis of corn stover and scum for bio-oil production with CaO and HZSM-5 as the catalyst. *Bioresour. Technol.* **2016**, *204*, 164–170. [[CrossRef](#)] [[PubMed](#)]
53. Park, H.J.; Heo, H.S.; Jeon, J.K.; Kim, J.; Ryoo, R.; Jeong, K.E.; Park, Y.K. Highly valuable chemicals production from catalytic upgrading of radiata pine sawdust-derived pyrolytic vapors over mesoporous MFI zeolites. *Appl. Catal. B* **2010**, *95*, 365–373. [[CrossRef](#)]
54. Yoo, M.L.; Park, Y.H.; Park, Y.K.; Park, S.H. Catalytic Pyrolysis of Wild Reed over a Zeolite-Based Waste Catalyst. *Energies* **2016**, *9*, 201. [[CrossRef](#)]
55. Wang, D.; Xiao, R.; Zhang, H.; He, G. Comparison of catalytic pyrolysis of biomass with MCM-41 and CaO catalysts by using TGA-FTIR analysis. *J. Anal. Appl. Pyrolysis* **2010**, *89*, 171–177. [[CrossRef](#)]
56. Stefanidis, S.D.; Kalogiannis, K.G.; Iliopoulou, E.F.; Lappas, A.A.; Pilavachi, P.A. In-situ upgrading of biomass pyrolysis vapors: catalyst screening on a fixed bed reactor. *Bioresour. Technol.* **2011**, *102*, 8261–8267. [[CrossRef](#)] [[PubMed](#)]
57. Stefanidis, S.D.; Karakoulia, S.A.; Kalogiannis, K.G.; Iliopoulou, E.F.; Delimitis, A.; Yiannoulakis, H.; Zampetakis, T.; Lappas, A.A.; Triantafyllidis, K.S. Natural magnesium oxide (MgO) catalysts: A cost-effective sustainable alternative to acid zeolites for the in situ upgrading of biomass fast pyrolysis oil. *Appl. Catal. B* **2016**, *196*, 155–173. [[CrossRef](#)]
58. Lim, X.Y.; Andresen, J.M. Pyro-catalytic deoxygenated bio-oil from palm oil empty fruit bunch and fronds with boric oxide in a fixed-bed reactor. *Fuel Process. Technol.* **2011**, *92*, 1796–1804. [[CrossRef](#)]
59. Imran, A.; Bramer, E.A.; Seshan, K.; Brem, G. High quality bio-oil from catalytic flash pyrolysis of lignocellulosic biomass over alumina-supported sodium carbonate. *Fuel Process. Technol.* **2014**, *127*, 72–79. [[CrossRef](#)]
60. Karnjanakom, S.; Bayu, A.; Hao, X.; Kongparakul, S.; Samart, C.; Abudula, A.; Guan, G. Selectively catalytic upgrading of bio-oil to aromatic hydrocarbons over Zn, Ce or Ni-doped mesoporous rod-like alumina catalysts. *J. Mol. Catal. A Chem.* **2016**, *421*, 235–244. [[CrossRef](#)]
61. Lu, Q.; Zhang, Z.F.; Dong, C.Q.; Zhu, X.F. Catalytic upgrading of biomass fast pyrolysis vapors with nano metal oxides: an analytical Py-GC/MS study. *Energies* **2010**, *3*, 1805–1820. [[CrossRef](#)]
62. Zheng, Y.; Chen, D.; Zhu, X. Aromatic hydrocarbon production by the online catalytic cracking of lignin fast pyrolysis vapors using  $\text{Mo}_2\text{N}/\gamma\text{-Al}_2\text{O}_3$ . *J. Anal. Appl. Pyrolysis* **2013**, *104*, 514–520. [[CrossRef](#)]
63. Zhou, L.; Yang, H.; Wu, H.; Wang, M.; Cheng, D. Catalytic pyrolysis of rice husk by mixing with zinc oxide: characterization of bio-oil and its rheological behavior. *Fuel Process. Technol.* **2013**, *106*, 385–391. [[CrossRef](#)]
64. Veses, A.; Aznar, M.; López, J.M.; Callén, M.S.; Murillo, R.; García, T. Production of upgraded bio-oils by biomass catalytic pyrolysis in an auger reactor using low cost materials. *Fuel* **2015**, *141*, 17–22. [[CrossRef](#)]
65. Aysu, T.; Sanna, A. Nannochloropsis algae pyrolysis with ceria-based catalysts for production of high-quality bio-oils. *Bioresour. Technol.* **2015**, *194*, 108–116. [[CrossRef](#)] [[PubMed](#)]

66. De Rezende Pinho, A.; de Almeida, M.B.; Mendes, F.L.; Ximenes, V.L.; Casavechia, L.C. Co-processing raw bio-oil and gasoil in an FCC unit. *Fuel Process. Technol.* **2015**, *131*, 159–166. [[CrossRef](#)]
67. Zhang, Z.B.; Lu, Q.; Ye, X.N.; Li, W.T.; Hu, B.; Dong, C.Q. Production of phenolic-rich bio-oil from catalytic fast pyrolysis of biomass using magnetic solid base catalyst. *Energy Convers. Manag.* **2015**, *106*, 1309–1317. [[CrossRef](#)]
68. Bu, Q.; Lei, H.; Wang, L.; Yadavalli, G.; Wei, Y.; Zhang, X.; Zhu, L.; Liu, Y. Biofuel production from catalytic microwave pyrolysis of Douglas fir pellets over ferrum-modified activated carbon catalyst. *J. Anal. Appl. Pyrolysis* **2015**, *112*, 74–79. [[CrossRef](#)]
69. Uzun, B.B.; Sarioğlu, N. Rapid and catalytic pyrolysis of corn stalks. *Fuel Process. Technol.* **2009**, *90*, 705–716. [[CrossRef](#)]
70. Kim, J.W.; Joo, S.H.; Seo, B.; Kim, S.S.; Shin, D.H.; Park, S.H.; Jeon, J.K.; Park, Y.K. Bio-Oil Upgrading via Catalytic Pyrolysis of Waste Mandarin Residue Over SBA-15 Catalysts. *J. Nanosci. Nanotechnol.* **2013**, *13*, 2566–2572. [[CrossRef](#)] [[PubMed](#)]
71. Wang, S.; Chen, J.; Cai, Q.; Zhang, F.; Wang, Y.; Ru, B.; Wang, Q. The effect of mild hydrogenation on the catalytic cracking of bio-oil for aromatic hydrocarbon production. *Int. J. Hydrog. Energy* **2016**, *41*, 16385–16393. [[CrossRef](#)]
72. Zhao, X.; Wei, L.; Cheng, S.; Julson, J.; Anderson, G.; Muthukumarappan, K.; Qiu, C. Development of hydrocarbon biofuel from sunflower seed and sunflower meat oils over ZSM-5. *J. Renew. Sustain. Energy* **2016**, *8*, 013109. [[CrossRef](#)]
73. Vitolo, S.; Bresci, B.; Seggiani, M.; Gallo, M.G. Catalytic upgrading of pyrolytic oils over HZSM-5 zeolite: behaviour of the catalyst when used in repeated upgrading–regenerating cycles. *Fuel* **2001**, *80*, 17–26. [[CrossRef](#)]
74. Wang, J.; Zhong, Z.; Ding, K.; Xue, Z. Catalytic fast pyrolysis of mushroom waste to upgraded bio-oil products via pre-coked modified HZSM-5 catalyst. *Bioresour. Technol.* **2016**, *212*, 6–10. [[CrossRef](#)] [[PubMed](#)]
75. Ibáñez, M.; Valle, B.; Bilbao, J.; Gayubo, A.G.; Castaño, P. Effect of operating conditions on the coke nature and HZSM-5 catalysts deactivation in the transformation of crude bio-oil into hydrocarbons. *Catal. Today* **2012**, *195*, 106–113. [[CrossRef](#)]
76. Valle, B.; Castaño, P.; Olazar, M.; Bilbao, J.; Gayubo, A.G. Deactivating species in the transformation of crude bio-oil with methanol into hydrocarbons on a HZSM-5 catalyst. *J. Catal.* **2012**, *285*, 304–314. [[CrossRef](#)]
77. Guisnet, M.; Costa, L.; Ribeiro, F.R. Prevention of zeolite deactivation by coking. *J. Mol. Catal. A Chem.* **2009**, *305*, 69–83. [[CrossRef](#)]
78. Guisnet, M.; Magnoux, P. Organic chemistry of coke formation. *Appl. Catal. A* **2001**, *212*, 83–96. [[CrossRef](#)]
79. Valle, B.; Gayubo, A.G.; Aguayo, A.T.; Olazar, M.; Bilbao, J. Selective production of aromatics by crude bio-oil valorization with a nickel-modified HZSM-5 zeolite catalyst. *Energy Fuels* **2010**, *24*, 2060–2070. [[CrossRef](#)]
80. Gayubo, A.G.; Valle, B.; Aguayo, A.T.; Olazar, M.; Bilbao, J. Olefin production by catalytic transformation of crude bio-oil in a two-step process. *Ind. Eng. Chem. Res.* **2009**, *49*, 123–131. [[CrossRef](#)]
81. Cerqueira, H.S.; Caeiro, G.; Costa, L.; Ribeiro, F.R. Deactivation of FCC catalysts. *J. Mol. Catal. A Chem.* **2008**, *292*, 1–13. [[CrossRef](#)]
82. Graça, I.; Carmo, A.M.; Lopes, J.M.; Ribeiro, M.F. Improving HZSM-5 resistance to phenolic compounds for the bio-oils/FCC feedstocks co-processing. *Fuel* **2015**, *140*, 484–494. [[CrossRef](#)]
83. Fogassy, G.; Thegarid, N.; Schuurman, Y.; Mirodatos, C. From biomass to bio-gasoline by FCC co-processing: effect of feed composition and catalyst structure on product quality. *Energy Environ. Sci.* **2011**, *4*, 5068–5076. [[CrossRef](#)]
84. Li, X.; Li, J.; Zhou, G.; Feng, Y.; Wang, Y.; Yu, G.; Deng, S.; Huang, J.; Wang, B. Enhancing the production of renewable petrochemicals by co-feeding of biomass with plastics in catalytic fast pyrolysis with ZSM-5 zeolites. *Appl. Catal. A* **2014**, *481*, 173–182. [[CrossRef](#)]
85. Zhu, X.; Mallinson, R.G.; Resasco, D.E. Role of transalkylation reactions in the conversion of anisole over HZSM-5. *Appl. Catal. A* **2010**, *379*, 172–181. [[CrossRef](#)]
86. Sharma, R.K.; Bakhshi, N.N. Catalytic upgrading of pyrolysis oil. *Energy Fuels* **1993**, *7*, 306–314. [[CrossRef](#)]
87. Sharma, R.K.; Bakhshi, N.N. Catalytic conversion of fast pyrolysis oil to hydrocarbon fuels over HZSM-5 in a dual reactor system. *Biomass Bioenergy* **1993**, *5*, 445–455. [[CrossRef](#)]

88. Gayubo, A.G.; Valle, B.; Aguayo, A.T.; Olazar, M.; Bilbao, J. Pyrolytic lignin removal for the valorization of biomass pyrolysis crude bio-oil by catalytic transformation. *J. Chem. Technol. Biotechnol.* **2010**, *85*, 132–144. [[CrossRef](#)]
89. Valle, B.; Gayubo, A.G.; Alonso, A.; Aguayo, A.T.; Bilbao, J. Hydrothermally stable HZSM-5 zeolite catalysts for the transformation of crude bio-oil into hydrocarbons. *Appl. Catal. B* **2010**, *100*, 318–327. [[CrossRef](#)]
90. Argyle, M.D.; Bartholomew, C.H. Heterogeneous catalyst deactivation and regeneration: A review. *Catalysts* **2015**, *5*, 145–269. [[CrossRef](#)]
91. Luo, Y.; Guda, V.K.; Steele, P.H.; Mitchell, B.; Yu, F. Hydrodeoxygenation of oxidized distilled bio-oil for the production of gasoline fuel type. *Energy Convers. Manag.* **2016**, *112*, 319–327. [[CrossRef](#)]
92. Cheng, S.; Wei, L.; Zhao, X.; Kadis, E.; Cao, Y.; Julson, J.; Gu, Z. Hydrodeoxygenation of prairie cordgrass bio-oil over Ni based activated carbon synergistic catalysts combined with different metals. *New Biotechnol.* **2016**, *33*, 440–448. [[CrossRef](#)] [[PubMed](#)]
93. Yang, T.; Jie, Y.; Li, B.; Kai, X.; Yan, Z.; Li, R. Catalytic hydrodeoxygenation of crude bio-oil over an unsupported bimetallic dispersed catalyst in supercritical ethanol. *Fuel Process. Technol.* **2016**, *148*, 19–27. [[CrossRef](#)]
94. Oh, S.; Hwang, H.; Choi, H.S.; Choi, J.W. Investigation of chemical modifications of micro-and macromolecules in bio-oil during hydrodeoxygenation with Pd/C catalyst in supercritical ethanol. *Chemosphere* **2014**, *117*, 806–814. [[CrossRef](#)] [[PubMed](#)]
95. Mortensen, P.M.; Gardini, D.; Damsgaard, C.D.; Grunwaldt, J.D.; Jensen, P.A.; Wagner, J.B.; Jensen, A.D. Deactivation of Ni-MoS<sub>2</sub> by bio-oil impurities during hydrodeoxygenation of phenol and octanol. *Appl. Catal. A* **2016**, *523*, 159–170. [[CrossRef](#)]
96. Kadarwati, S.; Hu, X.; Gunawan, R.; Westerhof, R.; Gholizadeh, M.; Hasan, M.M.; Li, C.Z. Coke formation during the hydrotreatment of bio-oil using NiMo and CoMo catalysts. *Fuel Process. Technol.* **2016**, *155*, 261–268. [[CrossRef](#)]
97. Hong, Y.K.; Lee, D.W.; Eom, H.J.; Lee, K.Y. The catalytic activity of Sulfided Ni/W/TiO<sub>2</sub> (anatase) for the hydrodeoxygenation of Guaiacol. *J. Mol. Catal. A Chem.* **2014**, *392*, 241–246. [[CrossRef](#)]
98. Oh, S.; Kim, U.J.; Choi, I.G.; Choi, J.W. Solvent effects on improvement of fuel properties during hydrodeoxygenation process of bio-oil in the presence of Pt/C. *Energy* **2016**, *113*, 116–123. [[CrossRef](#)]
99. Huang, Y.; Wei, L.; Zhao, X.; Cheng, S.; Julson, J.; Cao, Y.; Gu, Z. Upgrading pine sawdust pyrolysis oil to green biofuels by HDO over zinc-assisted Pd/C catalyst. *Energy Convers. Manag.* **2016**, *115*, 8–16. [[CrossRef](#)]
100. Dwiatmoko, A.A.; Zhou, L.; Kim, I.; Choi, J.W.; Suh, D.J.; Ha, J.M. Hydrodeoxygenation of lignin-derived monomers and lignocellulose pyrolysis oil on the carbon-supported Ru catalysts. *Catal. Today* **2016**, *265*, 192–198. [[CrossRef](#)]
101. Wang, Y.; He, T.; Liu, K.; Wu, J.; Fang, Y. From biomass to advanced bio-fuel by catalytic pyrolysis/hydro-processing: hydrodeoxygenation of bio-oil derived from biomass catalytic pyrolysis. *Bioresour. Technol.* **2012**, *108*, 280–284. [[CrossRef](#)] [[PubMed](#)]
102. Lee, E.H.; Park, R.S.; Kim, H.; Park, S.H.; Jung, S.C.; Jeon, J.K.; Kim, S.C.; Park, Y.K. Hydrodeoxygenation of guaiacol over Pt loaded zeolitic materials. *J. Ind. Eng. Chem.* **2016**, *37*, 18–21. [[CrossRef](#)]
103. Hellinger, M.; Baier, S.; Mortensen, P.M.; Kleist, W.; Jensen, A.D.; Grunwaldt, J.D. Continuous Catalytic Hydrodeoxygenation of Guaiacol over Pt/SiO<sub>2</sub> and Pt/H-MFI-90. *Catalysts* **2015**, *5*, 1152–1166. [[CrossRef](#)]
104. Xu, X.; Zhang, C.; Zhai, Y.; Liu, Y.; Zhang, R.; Tang, X. Upgrading of bio-oil using supercritical 1-Butanol over a Ru/C heterogeneous catalyst: role of the solvent. *Energy Fuels* **2014**, *28*, 4611–4621. [[CrossRef](#)]
105. Huynh, T.M.; Armbruster, U.; Atia, H.; Bentrup, U.; Phan, B.M.Q.; Eckelt, R.; Nguyen, L.H.; Nguyen, D.A.; Martin, A. Upgrading of bio-oil and subsequent co-processing under FCC conditions for fuel production. *React. Chem. Eng.* **2016**, *1*, 239–251. [[CrossRef](#)]
106. Ahmadi, S.; Yuan, Z.; Rohani, S.; Xu, C.C. Effects of nano-structured CoMo catalysts on hydrodeoxygenation of fast pyrolysis oil in supercritical ethanol. *Catal. Today* **2016**, *269*, 182–194. [[CrossRef](#)]
107. Zhang, X.; Wang, T.; Ma, L.; Zhang, Q.; Jiang, T. Hydrotreatment of bio-oil over Ni-based catalyst. *Bioresour. Technol.* **2013**, *127*, 306–311. [[CrossRef](#)] [[PubMed](#)]
108. Shafaghat, H.; Rezaei, P.S.; Daud, W.M.A.W. Catalytic hydrodeoxygenation of simulated phenolic bio-oil to cycloalkanes and aromatic hydrocarbons over bifunctional metal/acid catalysts of Ni/HBeta, Fe/HBeta and NiFe/HBeta. *J. Ind. Eng. Chem.* **2016**, *35*, 268–276. [[CrossRef](#)]

109. Wang, L.; Ye, P.; Yuan, F.; Li, S.; Ye, Z. Liquid phase in-situ hydrodeoxygenation of bio-derived phenol over Raney Ni and Nafion/SiO<sub>2</sub>. *Int. J. Hydrog. Energy* **2015**, *40*, 14790–14797. [[CrossRef](#)]
110. Sankaranarayanan, T.M.; Berenguer, A.; Ochoa-Hernández, C.; Moreno, I.; Jana, P.; Coronado, J.M.; Serrano, D.P.; Pizarro, P. Hydrodeoxygenation of anisole as bio-oil model compound over supported Ni and Co catalysts: Effect of metal and support properties. *Catal. Today* **2015**, *243*, 163–172. [[CrossRef](#)]
111. Ambursa, M.M.; Ali, T.H.; Lee, H.V.; Sudarsanam, P.; Bhargava, S.K.; Hamid, S.B.A. Hydrodeoxygenation of dibenzofuran to bicyclic hydrocarbons using bimetallic Cu–Ni catalysts supported on metal oxides. *Fuel* **2016**, *180*, 767–776. [[CrossRef](#)]
112. Mortensen, P.M.; Grunwaldt, J.D.; Jensen, P.A.; Jensen, A.D. Influence on nickel particle size on the hydrodeoxygenation of phenol over Ni/SiO<sub>2</sub>. *Catal. Today* **2016**, *259*, 277–284. [[CrossRef](#)]
113. Yang, Y.; Ochoa-Hernández, C.; Pizarro, P.; Víctor, A.; Coronado, J.M.; Serrano, D.P. Ce-promoted Ni/SBA-15 catalysts for anisole hydrotreating under mild conditions. *Appl. Catal. B* **2016**, *197*, 206–213. [[CrossRef](#)]
114. Xu, Y.; Li, Y.; Wang, C.; Wang, C.; Ma, L.; Wang, T.; Zhang, X.; Zhang, Q. In-situ hydrogenation of model compounds and raw bio-oil over Ni/CMK-3 catalyst. *Fuel Process. Technol.* **2016**. [[CrossRef](#)]
115. Xu, Y.; Wang, T.; Ma, L.; Zhang, Q.; Liang, W. Upgrading of the liquid fuel from fast pyrolysis of biomass over MoNi/γ-Al<sub>2</sub>O<sub>3</sub> catalysts. *Appl. Energy* **2010**, *87*, 2886–2891. [[CrossRef](#)]
116. Martínez, N.; García, R.; Fierro, J.L.G.; Wheeler, C.; Austin, R.N.; Gallagher, J.R.; Miller, J.T.; Krause, T.R.; Escalona, N.; Sepúlveda, C. Effect of Cu addition as a promoter on Re/SiO<sub>2</sub> catalysts in the hydrodeoxygenation of 2-methoxyphenol as a model bio oil compound. *Fuel* **2016**, *186*, 112–121. [[CrossRef](#)]
117. Tran, N.T.; Uemura, Y.; Chowdhury, S.; Ramli, A. Vapor-phase hydrodeoxygenation of guaiacol on Al-MCM-41 supported Ni and Co catalysts. *Appl. Catal. A* **2016**, *512*, 93–100. [[CrossRef](#)]
118. Sun, J.; Karim, A.M.; Zhang, H.; Kovarik, L.; Li, X.S.; Hensley, A.J.; McEwen, J.S.; Wang, Y. Carbon-supported bimetallic Pd–Fe catalysts for vapor-phase hydrodeoxygenation of guaiacol. *J. Catal.* **2013**, *306*, 47–57. [[CrossRef](#)]
119. Lai, Q.; Zhang, C.; Holles, J.H. Hydrodeoxygenation of Guaiacol over Ni@ Pd and Ni@ Pt Bimetallic Overlayer Catalysts. *Appl. Catal. A* **2016**, *528*, 1–13. [[CrossRef](#)]
120. Qiu, S.; Xu, Y.; Weng, Y.; Ma, L.; Wang, T. Efficient Hydrogenolysis of Guaiacol over Highly Dispersed Ni/MCM-41 Catalyst Combined with HZSM-5. *Catalysts* **2016**, *6*, 134. [[CrossRef](#)]
121. Zhang, X.; Wang, T.; Ma, L.; Zhang, Q.; Yu, Y.; Liu, Q. Characterization and catalytic properties of Ni and NiCu catalysts supported on ZrO<sub>2</sub>–SiO<sub>2</sub> for guaiacol hydrodeoxygenation. *Catal. Commun.* **2013**, *33*, 15–19. [[CrossRef](#)]
122. Han, Y.; McIlroy, D.N.; McDonald, A.G. Hydrodeoxygenation of pyrolysis oil for hydrocarbon production using nanospring based catalysts. *J. Anal. Appl. Pyrolysis* **2016**, *117*, 94–105. [[CrossRef](#)]
123. Duan, P.; Zhang, C.; Wang, F.; Fu, J.; Lü, X.; Xu, Y.; Shi, X. Activated carbons for the hydrothermal upgrading of crude duckweed bio-oil. *Catal. Today* **2016**, *274*, 73–81. [[CrossRef](#)]
124. Le, T.A.; Ly, H.V.; Kim, J.; Kim, S.S.; Choi, J.H.; Woo, H.C.; Othman, M.R. Hydrodeoxygenation of 2-furyl methyl ketone as a model compound in bio-oil from pyrolysis of Saccharina Japonica Alga in fixed-bed reactor. *Chem. Eng. J.* **2014**, *250*, 157–163. [[CrossRef](#)]
125. Ly, H.V.; Im, K.; Go, Y.; Galiwango, E.; Kim, S.S.; Kim, J.; Choi, J.H.; Woo, H.C. Spray pyrolysis synthesis of γ-Al<sub>2</sub>O<sub>3</sub> supported metal and metal phosphide catalysts and their activity in the hydrodeoxygenation of a bio-oil model compound. *Energy Convers. Manag.* **2016**, *127*, 545–553. [[CrossRef](#)]
126. Hakim, S.H.; Shanks, B.H.; Dumesic, J.A. Catalytic upgrading of the light fraction of a simulated bio-oil over CeZrO<sub>x</sub> catalyst. *Appl. Catal. B* **2013**, *142*, 368–376. [[CrossRef](#)]
127. Wang, W.; Yang, S.; Qiao, Z.; Liu, P.; Wu, K.; Yang, Y. Preparation of Ni–W–P–B amorphous catalyst for the hydrodeoxygenation of p-cresol. *Catal. Commun.* **2015**, *60*, 50–54. [[CrossRef](#)]
128. Peroni, M.; Mancino, G.; Baráth, E.; Gutiérrez, O.Y.; Lercher, J.A. Bulk and γ-Al<sub>2</sub>O<sub>3</sub>-supported Ni<sub>2</sub>P and MoP for hydrodeoxygenation of palmitic acid. *Appl. Catal. B* **2016**, *180*, 301–311. [[CrossRef](#)]
129. Boullosa-Eiras, S.; Lødeng, R.; Bergem, H.; Stöcker, M.; Hannevold, L.; Blekkan, E.A. Catalytic hydrodeoxygenation (HDO) of phenol over supported molybdenum carbide, nitride, phosphide and oxide catalysts. *Catal. Today* **2014**, *223*, 44–53. [[CrossRef](#)]
130. Yang, Y.; Gilbert, A.; Xu, C.C. Hydrodeoxygenation of bio-crude in supercritical hexane with sulfided CoMo and CoMoP catalysts supported on MgO: a model compound study using phenol. *Appl. Catal. A* **2009**, *360*, 242–249. [[CrossRef](#)]

131. Popov, A.; Kondratieva, E.; Mariey, L.; Goupil, J.M.; El Fallah, J.; Gilson, J.P.; Travert, A.; Maugé, F. Bio-oil hydrodeoxygenation: Adsorption of phenolic compounds on sulfided (Co)Mo catalysts. *J. Catal.* **2013**, *297*, 176–186. [[CrossRef](#)]
132. Gandarias, I.; Barrio, V.L.; Requies, J.; Arias, P.L.; Cambra, J.F.; Güemez, M.B. From biomass to fuels: Hydrotreating of oxygenated compounds. *Int. J. Hydrog. Energy* **2008**, *33*, 3485–3488. [[CrossRef](#)]
133. Horáček, J.; Kubička, D. Bio-oil hydrotreating over conventional CoMo & NiMo catalysts: The role of reaction conditions and additives. *Fuel* **2016**. [[CrossRef](#)]
134. He, Z.; Wang, X. Hydrodeoxygenation of model compounds and catalytic systems for pyrolysis bio-oils upgrading. *Catal. Sustain. Energy* **2012**, *1*, 28–52. [[CrossRef](#)]
135. Wildschut, J.; Mahfud, F.H.; Venderbosch, R.H.; Heeres, H.J. Hydrotreatment of fast pyrolysis oil using heterogeneous noble-metal catalysts. *Ind. Eng. Chem. Res.* **2009**, *48*, 10324–10334. [[CrossRef](#)]
136. Ardiyanti, A.R.; Gutierrez, A.; Honkela, M.L.; Krause, A.O.I.; Heeres, H.J. Hydrotreatment of wood-based pyrolysis oil using zirconia-supported mono- and bimetallic (Pt, Pd, Rh) catalysts. *Appl. Catal. A* **2011**, *407*, 56–66. [[CrossRef](#)]
137. Ardiyanti, A.R.; Khromova, S.A.; Venderbosch, R.H.; Yakovlev, V.A.; Heeres, H.J. Catalytic hydrotreatment of fast-pyrolysis oil using non-sulfided bimetallic Ni-Cu catalysts on a  $\delta$ -Al<sub>2</sub>O<sub>3</sub> support. *Appl. Catal. B* **2012**, *117*, 105–117. [[CrossRef](#)]
138. Leng, S.; Wang, X.; He, X.; Liu, L.; Liu, Y.E.; Zhong, X.; Zhuang, G.; Wang, J.G. NiFe/ $\gamma$ -Al<sub>2</sub>O<sub>3</sub>: A universal catalyst for the hydrodeoxygenation of bio-oil and its model compounds. *Catal. Commun.* **2013**, *41*, 34–37. [[CrossRef](#)]
139. Olcese, R.N.; Bettahar, M.; Petitjean, D.; Malaman, B.; Giovanella, F.; Dufour, A. Gas-phase hydrodeoxygenation of guaiacol over Fe/SiO<sub>2</sub> catalyst. *Appl. Catal. B* **2012**, *115*, 63–73. [[CrossRef](#)]
140. Wang, W.; Yang, Y.; Luo, H.; Hu, T.; Liu, W. Amorphous Co–Mo–B catalyst with high activity for the hydrodeoxygenation of bio-oil. *Catal. Commun.* **2011**, *12*, 436–440. [[CrossRef](#)]
141. Wang, W.; Yang, Y.; Luo, H.; Liu, W. Characterization and hydrodeoxygenation properties of Co promoted Ni–Mo–B amorphous catalysts: influence of Co content. *React. Kinet. Mech. Catal.* **2010**, *101*, 105–115. [[CrossRef](#)]
142. Zhang, W.; Zhang, Y.; Zhao, L.; Wei, W. Catalytic activities of NiMo carbide supported on SiO<sub>2</sub> for the hydrodeoxygenation of ethyl benzoate, acetone, and acetaldehyde. *Energy Fuels* **2010**, *24*, 2052–2059. [[CrossRef](#)]
143. Ghampson, I.T.; Sepúlveda, C.; Garcia, R.; Frederick, B.G.; Wheeler, M.C.; Escalona, N.; DeSisto, W.J. Guaiacol transformation over unsupported molybdenum-based nitride catalysts. *Appl. Catal. B* **2012**, *413*, 78–84. [[CrossRef](#)]
144. Koike, N.; Hosokai, S.; Takagaki, A.; Nishimura, S.; Kikuchi, R.; Ebitani, K.; Suzuki, Y.; Oyama, S.T. Upgrading of pyrolysis bio-oil using nickel phosphide catalysts. *J. Catal.* **2016**, *333*, 115–126. [[CrossRef](#)]
145. Lee, H.; Kim, Y.M.; Lee, I.G.; Jeon, J.K.; Jung, S.C.; Do Chung, J.; Choi, W.G.; Park, Y.K. Recent advances in the catalytic hydrodeoxygenation of bio-oil. *Korean J. Chem. Eng.* **2015**, 1–17. [[CrossRef](#)]
146. Mortensen, P.M.; Grunwaldt, J.D.; Jensen, P.A.; Knudsen, K.G.; Jensen, A.D. A review of catalytic upgrading of bio-oil to engine fuels. *Appl. Catal. A* **2011**, *407*, 1–19. [[CrossRef](#)]
147. Gao, D.; Schweitzer, C.; Hwang, H.T.; Varma, A. Conversion of guaiacol on noble metal catalysts: reaction performance and deactivation studies. *Ind. Eng. Chem. Res.* **2014**, *53*, 18658–18667. [[CrossRef](#)]
148. Popov, A.; Kondratieva, E.; Goupil, J.M.; Mariey, L.; Bazin, P.; Gilson, J.P.; Travert, A.; Maugé, F. Bio-oils hydrodeoxygenation: adsorption of phenolic molecules on oxidic catalyst supports. *J. Phys. Chem. C* **2010**, *114*, 15661–15670. [[CrossRef](#)]
149. Zanuttini, M.S.; Dalla Costa, B.O.; Querini, C.A.; Peralta, M.A. Hydrodeoxygenation of m-cresol with Pt supported over mild acid materials. *Appl. Catal. A* **2014**, *482*, 352–361. [[CrossRef](#)]
150. Furimsky, E.; Massoth, F.E. Deactivation of hydroprocessing catalysts. *Catal. Today* **1999**, *52*, 381–495. [[CrossRef](#)]
151. Echeandia, S.; Arias, P.L.; Barrio, V.L.; Pawelec, B.; Fierro, J.L.G. Synergy effect in the HDO of phenol over Ni–W catalysts supported on active carbon: Effect of tungsten precursors. *Appl. Catal. B* **2010**, *101*, 1–12. [[CrossRef](#)]
152. De La Puente, G.; Gil, A.; Pis, J.J.; Grange, P. Effects of support surface chemistry in hydrodeoxygenation reactions over CoMo/activated carbon sulfided catalysts. *Langmuir* **1999**, *15*, 5800–5806. [[CrossRef](#)]

153. Wang, B.; Duan, P.G.; Xu, Y.P.; Wang, F.; Shi, X.L.; Fu, J.; Lu, X.Y. Co-hydrotreating of algae and used engine oil for the direct production of gasoline and diesel fuels or blending components. *Energy* **2016**. [[CrossRef](#)]
154. Elliott, D.C.; Hart, T.R.; Neuenschwander, G.G.; Rotness, L.J.; Olarte, M.V.; Zacher, A.H.; Solantausta, Y. Catalytic hydroprocessing of fast pyrolysis bio-oil from pine sawdust. *Energy Fuels* **2012**, *26*, 3891–3896. [[CrossRef](#)]
155. Li, X.; Gunawan, R.; Wang, Y.; Chaiwat, W.; Hu, X.; Gholizadeh, M.; Mourant, D.; Bromly, J.; Li, C.Z. Upgrading of bio-oil into advanced biofuels and chemicals. Part III. Changes in aromatic structure and coke forming propensity during the catalytic hydrotreatment of a fast pyrolysis bio-oil with Pd/C catalyst. *Fuel* **2014**, *116*, 642–649. [[CrossRef](#)]
156. Jacobson, K.; Maheria, K.C.; Dalai, A.K. Bio-oil valorization: A review. *Renew. Sustain. Energy Rev.* **2013**, *23*, 91–106. [[CrossRef](#)]
157. Zhang, S.; Yan, Y.; Li, T.; Ren, Z. Upgrading of liquid fuel from the pyrolysis of biomass. *Bioresour. Technol.* **2005**, *96*, 545–550. [[CrossRef](#)] [[PubMed](#)]
158. Wang, F.; Li, M.L.; Duan, P.G.; Fu, J.; Lü, X.Y.; Xu, Y.P. Co-hydrotreating of used engine oil and the low-boiling fraction of bio-oil blends for the production of liquid fuel. *Fuel Process. Technol.* **2016**, *146*, 62–69. [[CrossRef](#)]
159. Chen, W.; Luo, Z.; Yu, C.; Li, G.; Yang, Y.; Zhang, H. Upgrading of bio-oil in supercritical ethanol: Catalysts screening, solvent recovery and catalyst stability study. *J. Supercrit. Fluids* **2014**, *95*, 387–393. [[CrossRef](#)]



© 2016 by the authors; licensee MDPI, Basel, Switzerland. This article is an open access article distributed under the terms and conditions of the Creative Commons Attribution (CC-BY) license (<http://creativecommons.org/licenses/by/4.0/>).